

Synthetic photometry from ATLAS9 models in the UB_V Johnson system

Fiorella Castelli

CNR-Gruppo Nazionale Astronomia and Osservatorio Astronomico, Via G. Tiepolo 11, I-34131 Trieste, Italy

Received 22 December 1998 / Accepted 18 March 1999

Abstract. Several grids of synthetic UB_V color indices computed in the Johnson system and based on ATLAS9 atmospheric models are compared and discussed.

We present synthetic colors which differ from those computed by Kurucz (1995) only for the convective models and for a very small shift of the zero-points. We compare these colors, called C97, with colors computed by Kurucz (1993a), Kurucz (1995) (K95), Bessell et al. (1998) (BCP). The Buser & Kurucz (1992) (BK92) colors, derived from models different from ATLAS9, are also considered. $T_{\text{eff}}-(U-B)$, $T_{\text{eff}}-(B-V)$, and $T_{\text{eff}}-BC_V$ relations are compared together and are compared with empirical relations from literature.

For convective stars ($T_{\text{eff}} \leq 8750$ K), ΔT_{eff} differences related with the different synthetic grids based on the ATLAS9 models are not larger than 100 K for $[M/H] = 0.0$ and 200 K for $[M/H] = -2.0$.

All the K95, C97, and BCP grids give, in general, T_{eff} larger than those from the empirical T_{eff} -color relations. For dwarfs, at $T_{\text{eff}} = 5000$ K and for $[M/H] = 0.0$, ΔT_{eff} from (U-B) is about 250 K, and ΔT_{eff} from (B-V) is on the order of 200 K. For giants, computed and observed $T_{\text{eff}}-(U-B)$ data agree well, while, for (B-V), the behaviour is similar to that for dwarfs. These results do not change in a significant way for different metallicities.

Computations performed for $[M/H] = -2.0$ have shown that, for dwarfs, the agreement with the observations improves when models computed for solar scaled abundances, but with α elements enhanced by 0.4 dex and based on the new solar iron abundance $\log(N_{Fe}/N_{tot}) = -4.53$ dex, are used.

The dependence of the color indices on T_{eff} , gravity, metallicity, and microturbulent velocity is investigated.

Key words: techniques: photometric – stars: atmospheres – stars: fundamental parameters

1. Introduction

Broad band color indices and bolometric corrections are usually used to transform from theoretical HR diagrams (luminosity vs.

T_{eff}) to observed magnitude color diagrams. Theoretical color-temperature and color-bolometric correction relations may be used to extend the range in T_{eff} , $\log g$, and metallicity covered by the empirical relations. Furthermore, color indices may be used to fix model parameters for stellar abundances determinations.

Starting from the seventies, Kurucz published extensive grids of models and colors, which have been improved over the years. In particular, UB_V colors computed in the Johnson system and based on Kurucz models or on Kurucz opacities were discussed by Buser & Kurucz (1978), Buser & Kurucz (1992), Kurucz (1991), Lejeune et al. (1997), and Bessell et al. (1998).

The early Buser & Kurucz (1978) UB_V grids, covering a range in T_{eff} from 5500 K to 50000 K, were later extended by Buser & Kurucz (1992) to lower temperatures ranging from 3750 K to 6000 K. Because, at that time, no models cooler than 5500 K were computed by Kurucz, owing to the lack of molecular opacities, Buser & Kurucz (1992) (BK92) adopted the cool models computed by Gustafsson et al. (1975), Bell et al. (1976), and Eriksson et al. (1979) and computed fluxes by using ODF's based on the Kurucz & Peytremann (1975) line lists, in spite of the lack of any molecular blanketing. As stressed by BK92, those fluxes were “not physically fully self-consistent, and will doubtlessly be improved by future calculations based on the new models of G-K stars and the more extensive opacity tables for both atomic and molecular lines which are currently being completed by Kurucz (1991)”.

In fact, new models were published by Kurucz (1993a). They are based on new opacity distribution functions computed with an huge number of both atomic and molecular lines lying in the whole spectrum from 90 Å to 100000 Å. Preliminary UB_V colors computed by using these new models were presented by Kurucz (1992) and definitive colors were later published (Kurucz, 1993a). However, new generations of convective models were computed later on both by Kurucz (1995), who improved the convection treatment related with the overshooting and by Castelli, who adopted the classical mixing-length theory for the convection, having dropped the overshooting option used by Kurucz. Bessell et al. (1998) presented extended grids of broad-band colors, based on both ATLAS and NMARCS model atmospheres.

Send offprint requests to: F. Castelli

Correspondence to: castelli@ts.astro.it

Because Bessell et al. (1998) used UB_V passbands and zero-points different from those used by Buser & Kurucz (1978) and Buser & Kurucz (1992) we reconsider in this paper UB_V photometry in according with Buser & Kurucz formulation, so that a more direct comparison with the Buser & Kurucz and Kurucz's papers can be performed. Furthermore, we extend the discussion to colors computed for different metallicities [M/H] and different microturbulent velocities ξ .

Sects. 4, 5, and 6 summarize which models, filters, and zero-points are used to compute the Kurucz grids (K95), the Castelli grids (C97), and the Bessell et al. grids (BCP). In Sect. 7 we compare the different synthetic colors and estimate the effective temperature differences related with the different grids of colors.

In order to estimate which grid fits the observations best, we investigate in Sects. 10 and 11 the agreement between the several computed T_{eff} -color relations with the corresponding empirical T_{eff} -color calibrations presented in Sect. 9.

The dependence of the computed color indices on T_{eff} , gravity, [M/H], and microturbulent velocity ξ is discussed in Sect. 8 and Sect. 12.

We used models computed with a 1996 version of the ATLAS code. The ODF's are those provided by Kurucz (1993b). A Vega model (Castelli & Kurucz, 1994) consistent with all the updated computations was used to fix the zero-points.

All the grids discussed in this paper, except the Bessell et al. (1998) color indices, are available at: <http://cfaku5.harvard.edu>. The BCP color indices are available at CDS and on request.

2. Synthetic colors and bolometric corrections

Color indices are defined as the difference between the magnitudes of a star in two different spectral regions. The magnitudes are the apparent ones when the observed indices are considered, while they involve the flux at the stellar surface when synthetic indices are computed.

The computed magnitude m_i corresponding to a particular filter or passband i is:

$$m_i = -2.5 \log \int_{\alpha_i}^{\beta_i} F_{\lambda} S_i(\lambda) d\lambda \quad (1)$$

or

$$m_i = -2.5 \log \left[\int_{\alpha_i}^{\beta_i} F_{\lambda} S_i(\lambda) d\lambda / \int_{\alpha_i}^{\beta_i} S_i(\lambda) d\lambda \right] \quad (2)$$

where F_{λ} is the computed monochromatic flux at the star surface, $S_i(\lambda)$ is the response function of the photometric system in the i passband, and α_i and β_i define the wavelength interval of $S_i(\lambda)$.

Each computed index can then be related to the corresponding observed index by means of an additive constant, namely:

$$(m_i - m_j)_{\text{obs}} = (m_i - m_j)_{\text{calc}} + C \quad (3)$$

The constant C is derived by forcing a fit between computed and observed colors for a given star or a sample of stars well

reproduced by the atmospheric models. Vega is usually adopted to fix the constant, but also the color indices of a mean A0 V star are often used as zero-point for several observed standard systems.

The bolometric correction BC_i relative to a given magnitude is the correction required to reduce the color magnitude to the bolometric magnitude. The computed BC_i is given by

$$BC_i = (m_{\text{bol}} - m_i)_{\text{calc}} + K \quad (4)$$

where

$$m_{\text{bol}} = -2.5 \log \int_0^{\infty} \pi F_{\lambda} d\lambda \quad (5)$$

and the constant K is defined by the zero-point adopted to normalize the computed BC_i to the observed system.

Synthetic photometry is therefore conditioned by the model atmospheres through the flux F_{λ} , by the computed shape of the S_i functions representing the instrumental passbands, and by the adopted zero-points.

3. The UB_V synthetic grids

The grids of UB_V synthetic colors considered in this paper are those of Buser & Kurucz (1992) (BK92), Kurucz (1993) (K93), Kurucz (1995) (K95), Castelli (C97), and those in Bessell et al. (1998) (BCP) based on the ATLAS models computed with no overshooting in the mixing-length convection.

All the grids use model atmospheres computed from the ATLAS9 code, except BK92, which is based on the Gustafsson et al. (1975), Bell et al. (1976), and Eriksson et al. (1979) models. All the grids use synthetic fluxes computed with the line opacities (ODF's) including the molecular transitions (Kurucz, 1993b), except BK92 which uses ODF's derived from the Kurucz & Peytremann (1975) (KP) line list. The KP line list does not include molecular lines and it has many fewer atomic lines than those considered in the successive line lists provided by Kurucz.

The K93, K95, and C97 grids differ for the convection used for computing the models having T_{eff} between 3500 K and 8750 K. Furthermore, there is a slight difference in the zero-points between the K93, K95 grids on the one hand and the C97 grid on the other hand.

The BCP grids differ from the K93, K95, and C97 grids for both the passbands and the zero-points adopted for the (U-B) and (B-V) color indices and BC_V bolometric correction.

We now discuss in more detail each particular grid and the differences between the different grids.

4. Kurucz's UB_V synthetic photometry (K95)

4.1. The atmospheric models K93, K94, K95

Grids of colors computed by Kurucz are those published on the CD-ROM 13 (Kurucz, 1993a) and on the CD-ROM 19 (Kurucz, 1994) (K93 and K94). In the first case the colors are computed for 19 different metallicities ranging from [M/H] = +1.0

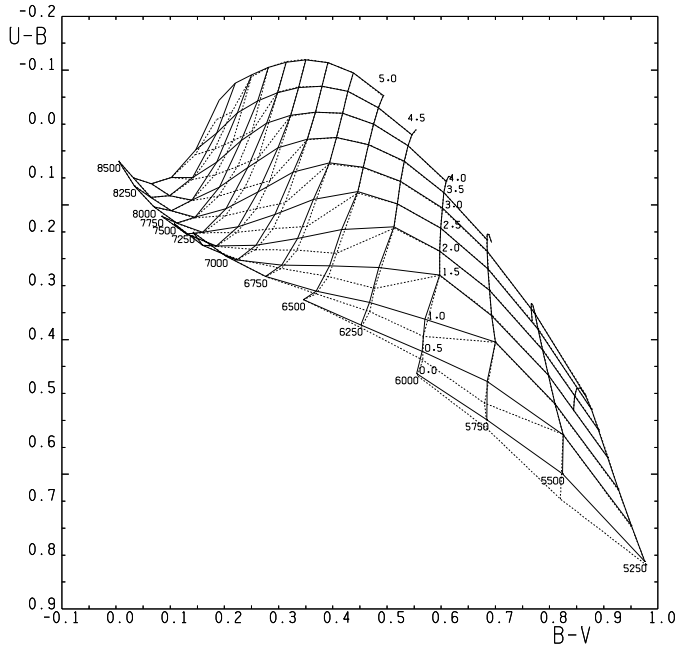


Fig. 1. Comparison of U-B, B-V relations from K93 (dashed lines) and K95 (full lines) models

to $[M/H] = -5.0$, but for only one microturbulent velocity $\xi = 2 \text{ km s}^{-1}$. In the second case the colors are computed for 5 different microturbulent velocities 0, 1, 2, 4, and 8 km s^{-1} , but for only one metallicity $[M/H] = 0.0$. The grid with $[M/H] = 0.0$ and $\xi = 2 \text{ km s}^{-1}$ is distributed in both CD-ROMs. The only difference is that the grid on CD-ROM 19 contains more numerous models.

The color-color relations derived from these grids showed discontinuities which do not appear in the corresponding observed relations. Castelli (1996) explained how to eliminate the color jumps which were related to a modification of the mixing-length convection adopted by Kurucz for computing the 1993 and 1994 models and called by him “approximate overshooting”. Owing to a conceptual error in the convection routine of ATLAS9, the models with zero convection at the bottom of the atmosphere ($\tau_{Ross} = 100$) were computed without any “overshooting” for the convection, while all the other convective models were computed with the “approximate overshooting”. The discontinuities occurred at the edges of the two regimes.

The convective models before 1995 were recomputed by Kurucz by adopting the improvement suggested by Castelli for the “approximate overshooting”. These are here called the K95 models.

Fig. 1 compares (U-B, B-V) grids computed from the K93 and K95 model atmospheres for $[M/H] = 0.0$ and $\xi = 2 \text{ km s}^{-1}$. The discontinuities are manifest in the K93 grid (dashed lines).

4.2. The passbands and zero-points

A complete description of the numerical procedure used by Kurucz to compute color indices and bolometric correction in the

UBV Johnson system can be found in Kurucz (1979), Buser & Kurucz (1978), and Buser & Kurucz (1992).

The UBVBUSER code, as distributed by Kurucz on the CD-ROM No 13, was used for computing the UB_V photometry. Input data is a grid of computed fluxes and output data are U, B, and V magnitudes (corresponding to the flux at the stellar surface), the color indices (U-B) and (B-V) normalized to the observed system, the bolometric correction BC_V relative to the V magnitude, and the quantity $BOL = -2.5 \log(\sigma T_{eff}^4 / \pi)$.

The U, B, and V magnitudes are defined with both formulas (1) and (2), but with $F(\lambda)$ replaced by the Eddington flux $H_\lambda = F_\lambda / 4$. The passbands $S_i(\lambda)$ are those of the Johnson & Morgan (1951) system reconstructed at Vilnius (Azusienis & Straizys, 1969), and modified by Buser (1978). The response function S_U for the U region (305–420 nm) is from Buser (1978), and the S_B and S_V functions for the B (360–455 nm) and V (475–740 nm) regions are from Azusienis & Straizys (1969). They take into account the extinction of the earth atmosphere by assuming $\sec z = 1.3$ for the U and B colors when the (U-B) index is computed and $\sec z = 0$ for the B and V colors when the (B-V) index is computed. z is the zenith angle.

Observed (U-B) and (B-V) indices of Vega are used to fix the zero-point of the synthetic photometric system. Kurucz (1979), Buser & Kurucz (1978), and Buser & Kurucz (1992) used an ATLAS6 Vega model with parameters $T_{eff} = 9400 \text{ K}$, $\log g = 3.95$, $[M/H] = 0.0$, and $\xi = 2 \text{ km s}^{-1}$. Kurucz (1992) used an ATLAS9 model with the same parameters and, finally, Kurucz (1993a) used the ATLAS9 model from Castelli & Kurucz (1994) with parameters $T_{eff} = 9550 \text{ K}$, $\log g = 3.95$, $[M/H] = -0.5$, and $\xi = 2 \text{ km s}^{-1}$.

Spectrophotometric observations from Straizys & Sviderskiene (1972) were used by Buser (1978) to obtain the following transformation equations from the reconstructed natural system $(U-B)_r$, $(B-V)_r$ and the standard UB_V Johnson-Morgan system:

$$(U - B) = (U - B)_r - 1.093 \quad (6)$$

$$(B - V) = (B - V)_r + 0.710 \quad (7)$$

The above relations are part of the UBVBUSER code and give $(U-B) = -0.016$ and $(B-V) = -0.015$ for Vega. The constant $C_{U-B} = +0.011$ and $C_{B-V} = +0.012$ were added to (6) and (7) in order to recover $(U-B) = -0.005$ and $(B-V) = -0.003$, assumed by Kurucz as observed indices of Vega.

4.3. The bolometric correction

In accordance with (4) and (5) the bolometric correction is:

$$BC_V = -2.5 \left[\log \sigma T_{eff}^4 / \pi - \log \int_{\alpha}^{\beta} S_V(\lambda) H(\lambda) d\lambda \right] + K \quad (8)$$

In this system, the constant K includes the constant $-2.5 \log(1/4)$ which is needed to convert the flux $F(\lambda)$ in $H(\lambda)$. K is defined by normalizing to zero the smallest bolometric correction (in absolute value) of the whole synthetic grid computed for $[M/H] = 0.0$ and microturbulent velocity $\xi = 2 \text{ km s}^{-1}$. It

Table 1. Bolometric corrections BC_V in the synthetic grids

Ref	BC(def.)	BC(5770 K,4.4377) model	BC adopted	BC _⊙ adopted	BC' _⊙ = -0.07
K (1979)	BOL-V'+6.986	-0.214	BC(def.)	-0.194	BC+0.124
BK(1978)	BOL*-V'+8.491	-0.214	BC(def.)+0.1	-0.094	BC+0.124
BK92	BOL-V'+6.986	-0.189	BC(def.)+0.1	-0.089	BC+0.119
K95	BOL*-V'+8.42	-0.193	BC(def.)	-0.193	BC+0.123
C97	BOL-V+2.124	-0.193	BC(def.)	-0.193	BC+0.123

$$\text{BOL} = -2.5 \log(\sigma T_{\text{eff}}^4 / \pi), \text{BOL}^* = -2.5 \log(\sigma T_{\text{eff}}^4 / 4\pi), V = -2.5 [\log \int_{\alpha_i}^{\beta_i} H_{\lambda} S_i(\lambda) d\lambda], V' = -2.5 \log \left[\frac{\int_{\alpha_i}^{\beta_i} H_{\lambda} S_i(\lambda) d\lambda}{\int_{\alpha_i}^{\beta_i} S_i(\lambda) d\lambda} \right]$$

occurs for the model $T_{\text{eff}} = 7250$ K, $\log g = 0.5$. With this normalization, positive values for BC_V are avoided. For the Sun, BC_{V⊙} = -0.193.

By assuming $V_{\odot} = -26.75$ (Hayes, 1985), the absolute magnitude is $M_{V_{\odot}} = 4.82$. Therefore, for the normalization adopted by Kurucz, $M_{\text{bol}_{\odot}}$ is given by $M_{V_{\odot}} + \text{BC}_{V_{\odot}} = 4.63$.

If, instead, BC'_{V⊙} = -0.07 is assumed as zero-point, all Kurucz's BC_V have to be rescaled. The conversion is:

$$\text{BC}'_V = \text{BC}_V + 0.123 \quad (9)$$

In fact:

$$\text{BC}'_{V_{\odot}} = -0.193 + 0.123 = -0.07 \quad (10)$$

In this case, $M_{\text{bol}_{\odot}}$ is given by $M_V + \text{BC}'_{V_{\odot}} = 4.75$, and all the bolometric magnitudes will be derived by using the BC'_V bolometric corrections (9).

Table 1 lists some values for bolometric corrections based on Kurucz models. Both Buser & Kurucz (1978) and Buser & Kurucz (1992) redefined the zero-points of BC_V derived from the models by increasing them by 0.1 mag, on the basis of a fit to the BC_V- T_{eff} empirical relation from Code et al. (1976). Column 5 of Table 1 shows that these renormalizations lowered the final solar BC_⊙ from -0.19 to -0.09.

5. Castelli UB_V synthetic photometry (C97)

5.1. The atmospheric models

ATLAS9 convective models computed without any overshooting were used. In fact, Castelli et al. (1997) discussed the differences on some color indices and Balmer profiles produced by the models computed both with and without “overshooting” and concluded that, except for the Sun, the no-overshoot models better agree with the observations, mostly for stars hotter than the Sun.

Castelli recomputed grids of convective models (T_{eff} 3500–8750 K) with metallicities $[M/H] = +0.5, 0.0, -0.5, -1.0, -1.5, -2.0,$ and -2.5 and microturbulent velocity $\xi = 2$ km s⁻¹. Furthermore, by using Kurucz's ODF's, she computed complete new grids (T_{eff} 3500–50000 K) for $[M/H] = -2.0a$ and $\xi = 1.0, 2.0, 4.0$ km s⁻¹, and $[M/H] = -1.0a, -1.5a$ and $\xi = 1.0$ km s⁻¹. The symbol “a” indicates abundances for the α elements (O, Ne, Mg, Si, S, Ar, Ca, and Ti) enhanced by 0.4 dex relative to the solar ones and solar iron abundance

$\log(N_{\text{Fe}}/N_{\text{tot}}) = -4.53$ (Holweger et al., 1995). For all the other grids solar and solar scaled abundances were used, in that the same ODF's used by Kurucz for computing the K93, K94, and K95 models were adopted. In this case, the solar iron abundance is -4.37 dex from Anders & Grevesse (1989). The lower value of the solar iron abundance from Holweger et al. (1995) should be preferred. In fact, it was later confirmed by Anstee, O' Mara & Ross (1997), who derived $\log(N_{\text{Fe}}/N_{\text{tot}}) = -4.53 \pm 0.01$ from the fit of 26 strong Fe I solar lines to lines computed with accurate laboratory gf values and collision damping constants computed according to the theory of Anstee & O' Mara (1995).

5.2. The passbands and zero-points

The UBVBUSER code was used to compute the U, B, V colors, so that we adopted the same passbands used by K95. However, (U-B) and (B-V) zero-points were slightly modified, in that we adopted (U-B) = 0.000 and (B-V) = 0.000 as observed indices of Vega, in according to Johnson et al. (1966). We called (B-V)(J) the indices with this normalization to distinguish them from those normalized on (B-V) = -0.016 for Vega, as derived by Hayes (1985) from the observed flux of Vega together with the Azusienis & Straizys (1969) response functions. We computed (B-V) indices also for this second normalization and called them (B-V)(H). We recall that Bessell (1983) measured for Vega (B-V) = -0.010.

For BC_V we adopted the same zero-point adopted by K95.

6. Bessell, Castelli & Plez UB_V synthetic photometry (BCP)

Bessell et al. (1998) published tables of colors based on both K95 and C97 models computed for solar metallicity. However, these colors are different from the previous ones because they are computed with different U, B, and V passbands and different zero-points.

6.1. The passbands

The UB_V magnitudes were computed by using the UB_V passbands from Bessell (1990). Furthermore, the computed (U-B) colors for O-K stars were then modified by multiplying them by 0.96 in order to force them to agree with a mean relation T_{eff} -

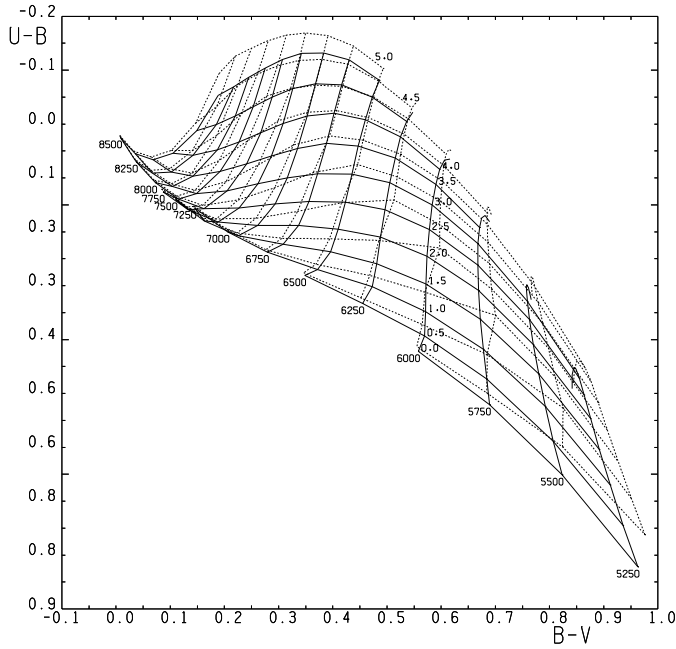


Fig. 2. Comparison of U-B, B-V relations from K95 (dashed lines) and C97 (full lines) models

(U-B) for O-B stars derived by combining T_{eff} -spectral type relations from Crowther (1997) and from Böhm-Vitense (1982) with (U-B)-spectral type relations from FitzGerald (1970).

A general discussion on the accuracy of the passbands adopted for synthetic photometry is given in Appendix E in the Bessell et al. (1998) paper.

6.2. The zero-points

Both Vega and Sirius were used to fix the zero-points of the (U-B) and (B-V) indices. Observed indices of Vega were assumed to be $(U-B) = 0.000$ (Johnson et al., 1966) and $(B-V) = -0.005$ (the average of $(B-V) = 0.000$ from Johnson et al. (1966) and $(B-V) = -0.010$ from Bessell (1990)). Observed indices of Sirius are $(U-B) = -0.045$ and $(B-V) = -0.010$ (Cousins, 1972). The Vega model is from Castelli & Kurucz (1994) and the Sirius model is from Kurucz (1997a). The parameters T_{eff} , $\log g$, $[M/H]$, and microturbulent velocity are (9550 K, 3.95, $[-0.5]$, 2 km s^{-1}) for the Vega model and (9850 K, 4.25, $[+0.4]$, 0 km s^{-1}) for the Sirius model. The differences between the observed and computed colors of Vega and the differences between the observed and computed colors of Sirius were averaged. The average difference was used to fix the zero-points.

6.3. Bolometric corrections

Bolometric correction BC_V was computed by adopting as zero-point $BC_V = -0.07 \text{ mag}$ for the Sun. It was derived by assuming the absolute bolometric magnitude of the Sun to be known and given by $M_{\text{bol}\odot} = 4.74 \text{ mag}$. For the observed V_{\odot} the value -26.76 mag was adopted.

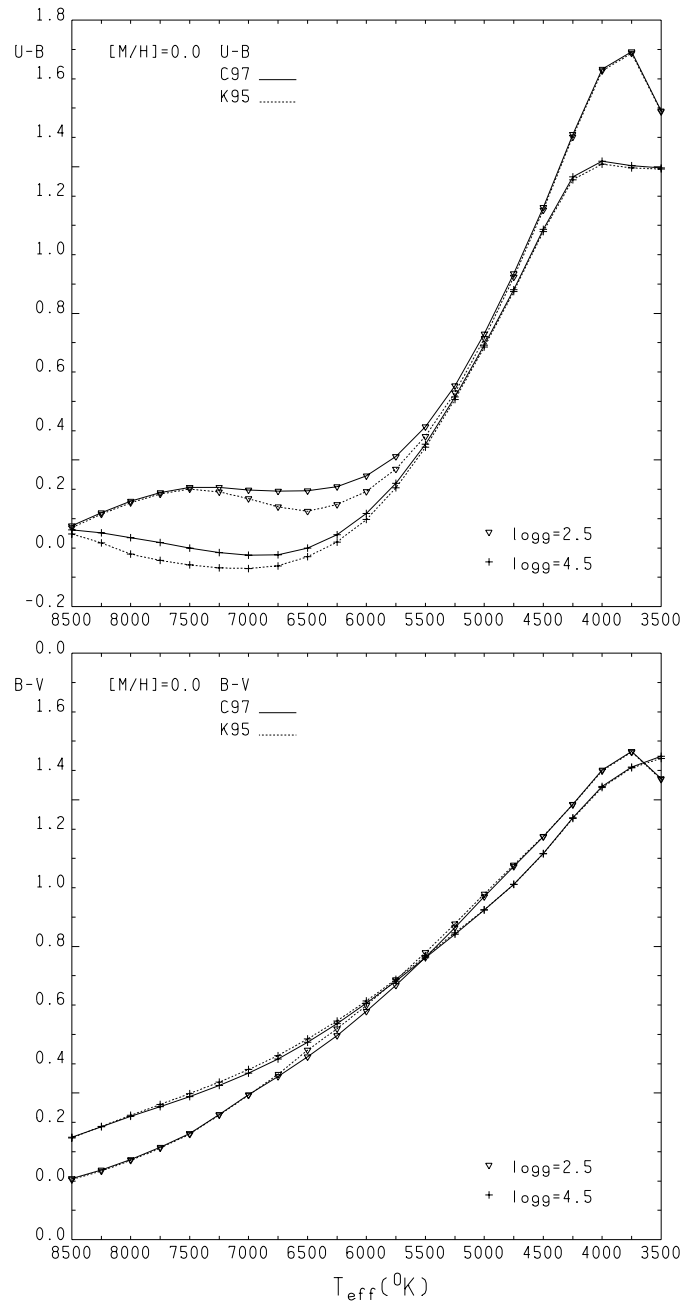


Fig. 3. Comparison of U-B, B-V from K95 (dashed lines) and C97 (full lines) as a function of T_{eff} for the two gravities $\log g = 2.5$ and $\log g = 4.5$

7. Comparison of color indices

7.1. K95 and C97 color indices

These indices differ only for the convection adopted in the models and for a slight difference in the zero-points. Fig. 2 compares (U-B, B-V) diagrams from K95 and C97 models for T_{eff} between 5500 K and 8500 K. Almost all colors are different in this range of T_{eff} .

Fig. 3 compares, for the two gravities $\log g = 4.5$ and $\log g = 2.5$, and $[M/H] = 0.0$, the (U-B) and (B-V) indices as a function

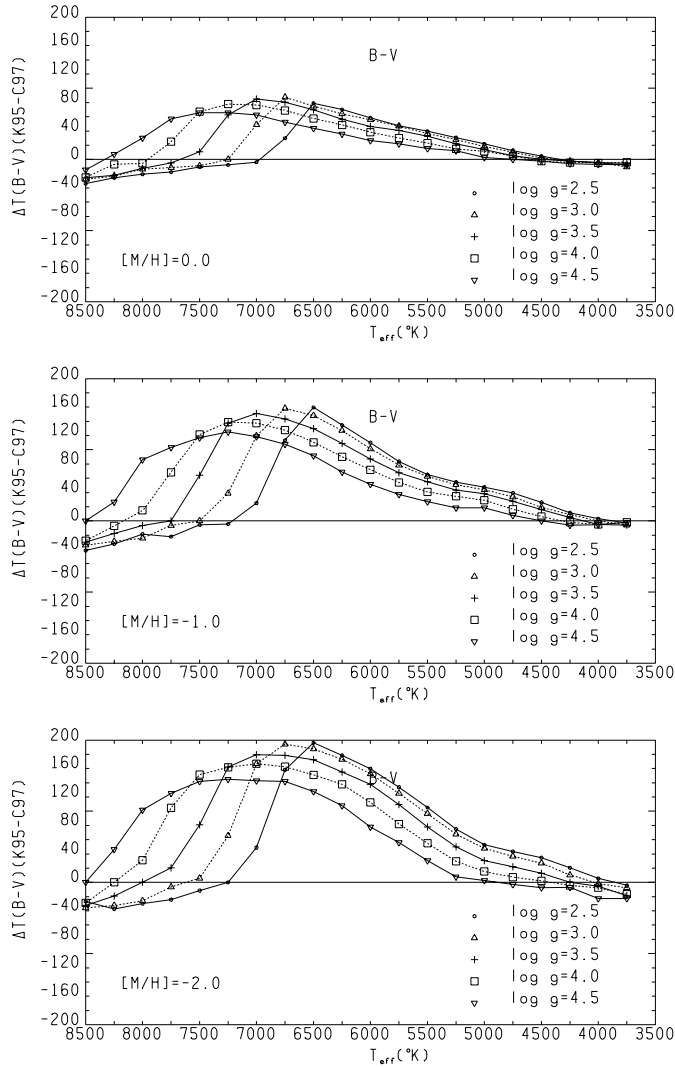


Fig. 4. ΔT_{eff} differences from C97 and K95 (B-V) indices for different gravities and metallicities

of T_{eff} from C97 and from K95. The differences are larger for (U-B) than for (B-V) and occur mostly for $T_{\text{eff}} > 5500$ K.

Fig. 4 quantifies the differences ΔT_{eff} as a function of T_{eff} for different metallicities when the (B-V) index is considered. The largest ΔT_{eff} differences increase from about 100 K for $[M/H] = 0.0$ to about 200 K for $[M/H] = -2.0$.

This kind of comparison is rather meaningless for the (U-B) index when $T_{\text{eff}} > 6000$ K, because (U-B) is independent of T_{eff} in this range of temperatures, as is evident from Fig. 3. The dependence of the color indices on T_{eff} is also discussed in Sect. 8.

A similar analysis performed on the BC_V bolometric corrections has shown that there are no differences between bolometric corrections computed from models with and without overshooting.

The comparison between the K95 and C97 color indices shows the effect of convection in the atmospheres of the cool stars. The influence of convection in ATLAS9 model atmospheres

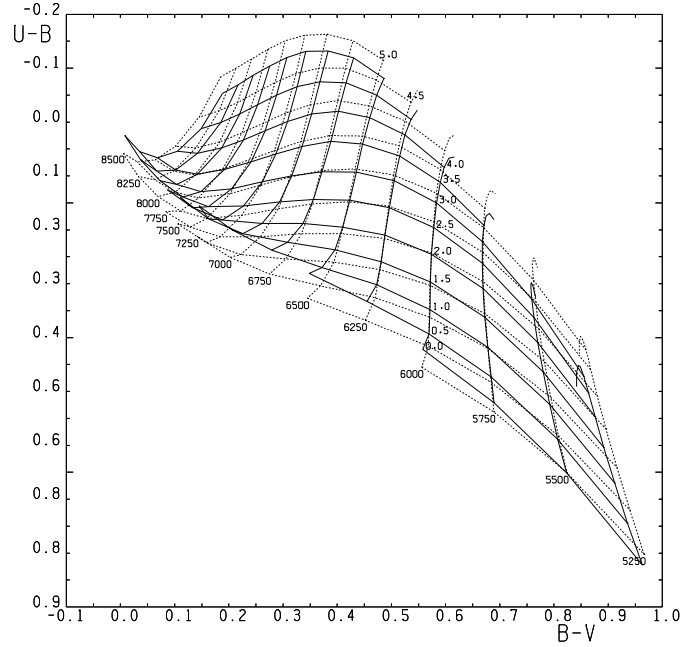


Fig. 5. Comparison of U-B, B-V relations from BCP (dashed lines) and C97 (full lines) models

was discussed in Castelli et al. (1997), while Kurucz (1997b) stressed the fact that every one-dimensional approximation for convective motions, like mixing-length, or mixing-length + overshooting, or the full spectrum of turbulence (FST) (Canuto & Mazzitelli, 1992), are all unrealistic treatments. In fact, convective motions are ascending and descending gaseous flows having different velocities and temperatures that very probably do not average into any one-dimensional treatment used up to now in the model atmosphere computations. Incorrect results are the consequence of the uni-dimensional approximation in the model atmospheres for the convective motions. The most evident discrepancies from the observations predicted by models and related to the unrealistic convection are listed in Kurucz (1997b).

7.2. BCP and C97 color indices

These indices differ for the adopted passbands and for the zero-points. They may also differ for the models if BCP colors from models computed with overshooting are considered. We discuss here only BCP colors from models without overshooting. Fig. 5 compares (U-B, B-V) diagrams from BCP and C97 for convective models and $T_{\text{eff}} > 5250$ K. All the colors are different.

Fig. 6 compares, for the two gravities $\log g = 4.5$ and $\log g = 2.5$, and for $[M/H] = 0.0$, the (U-B) and (B-V) indices as a function of T_{eff} from C97 and from BCP grids. The differences are larger for (U-B) than for (B-V). For (U-B) they are mostly due to the 0.96 multiplicative factor adopted by BCP (Sect. 6).

Fig. 7 quantifies the differences $\Delta T_{\text{eff}} = T_{\text{eff}}(\text{BCP}) - T_{\text{eff}}(\text{C97})$ as a function of T_{eff} for different metallicities when the (B-V) index is considered. The differences in (B-V) are very small and, for $[M/H] = 0.0$, ΔT_{eff} ranges from +20 K at $T_{\text{eff}} =$

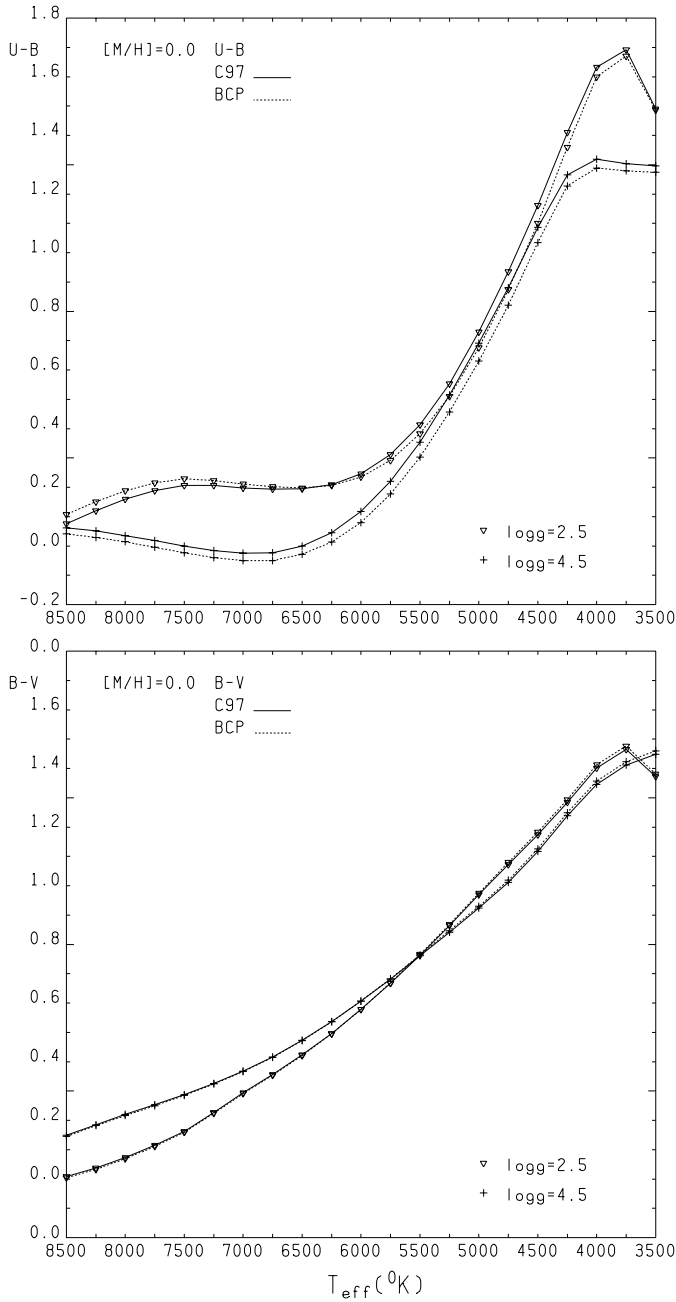


Fig. 6. Comparison of (U-B) and (B-V) from BCP (dashed lines) and C97 (full lines) as a function of T_{eff} for the two gravities $\log g = 2.5$ and $\log g = 4.5$

3750 K to -60 K at $T_{\text{eff}} = 8500$ K. These values are the same or even decrease with decreasing metallicity.

7.3. BCP and K95 color indices

These indices differ for passbands and zero-points. For $T_{\text{eff}} < 9000$ K they may also differ for the models when BCP colors from models without overshooting are considered. We discuss here only BCP colors from models without overshooting. Fig. 8 compares (U-B, B-V) diagrams for convective models for $T_{\text{eff}} >$

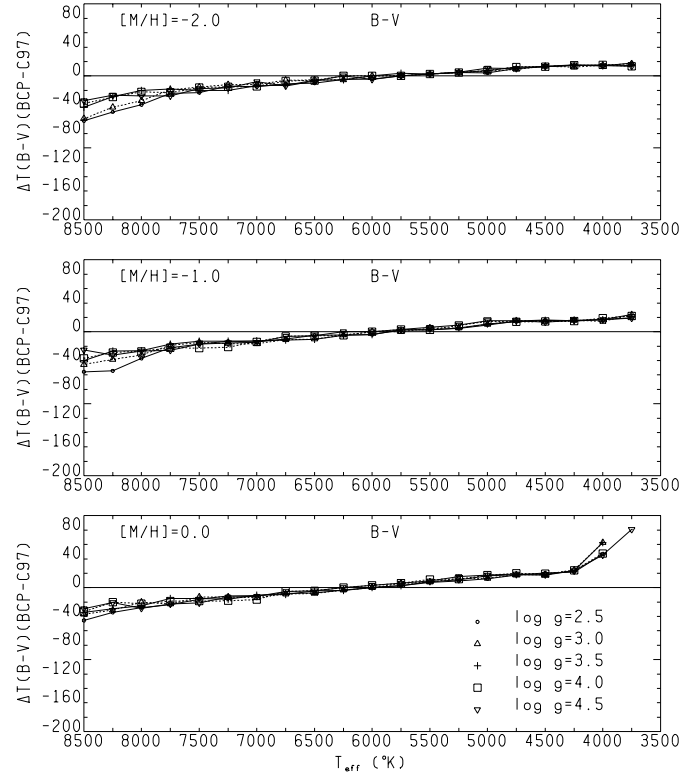


Fig. 7. ΔT_{eff} differences from BCP and C97 (B-V) indices for different gravities and metallicities

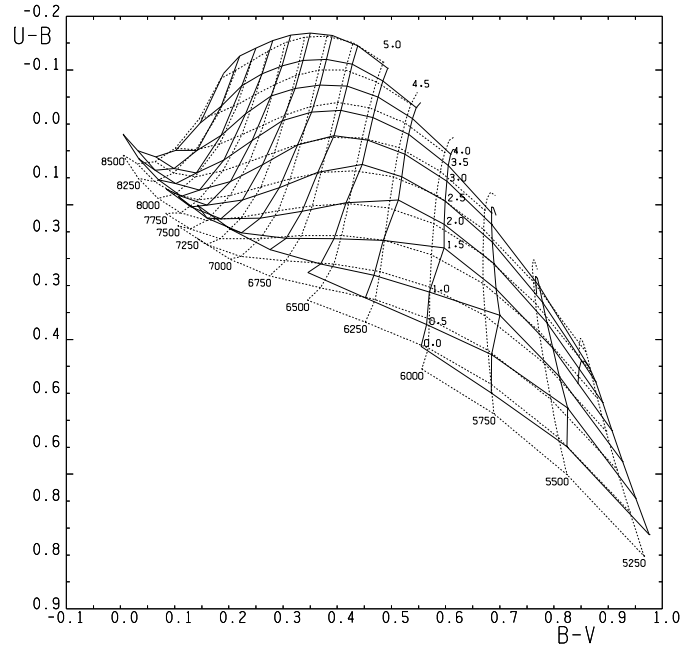


Fig. 8. Comparison of U-B, B-V relations from BCP (dashed lines) and K95 (full lines) models

5250 K and Fig. 9 compares, for the two gravities $\log g = 4.5$ and $\log g = 2.5$, and for $[M/H] = 0.0$, the (U-B) and (B-V) indices as a function of T_{eff} from BCP and from K95 grids.

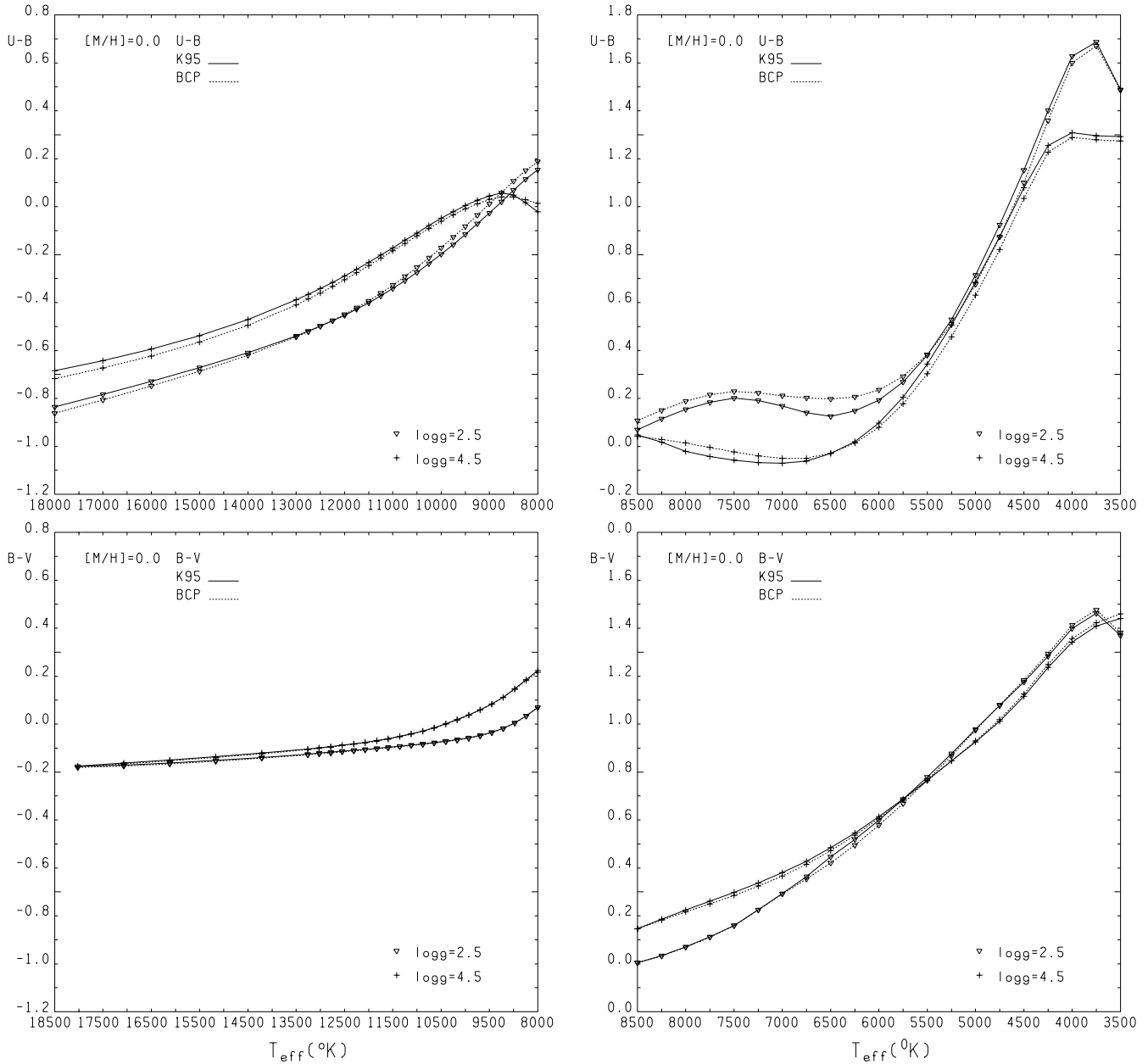


Fig. 9. Comparison of $T_{\text{eff}}\text{-(U-B)}$, $T_{\text{eff}}\text{-(B-V)}$ relations from BCP (dashed lines) and K95 (full lines) for the two gravities $\log g = 2.5$ and $\log g = 4.5$

While the differences in (B-V) indices are not very large, they are significant for (U-B).

There are no differences between BC_V bolometric corrections from BCP and K95 colors, once the same zero-point is assumed for both.

7.4. C97 and Buser & Kurucz (1992) (BK92) color indices

These indices differ for the models, the fluxes, and the Vega model. BK92 used models computed by Gustafsson et al. (1975), Bell et al. (1976), and Eriksson et al. (1979). The fluxes were computed by using ODF's based on the Kurucz & Peytremann (1975) line lists, which do not include molecular tran-

sitions. The Vega model used to normalize the colors was the ATLAS6 model with parameters $T_{\text{eff}} = 9400$ K, $\log g = 3.90$, $[M/H] = 0.0$, and $\xi = 2$ km s $^{-1}$.

Fig. 10 compares, for the two gravities $\log g = 4.5$ and $\log g = 1.5$, and $[M/H] = 0.0$, the (U-B) and (B-V) indices as a function of T_{eff} from BK92 and from C97 grids. For the same value of (U-B) or (B-V) T_{eff} from the C97 models are always larger than those from BK92. The difference is larger for (U-B) than for (B-V) and for both indices the difference increases with decreasing gravity. The plots on the right in Fig. 10 show the ΔT_{eff} differences as a function of T_{eff} when the same value for a given index is considered in the two grids. ΔT_{eff} differences are plotted for the three different gravities $\log g = 1.5$, 3.0, and

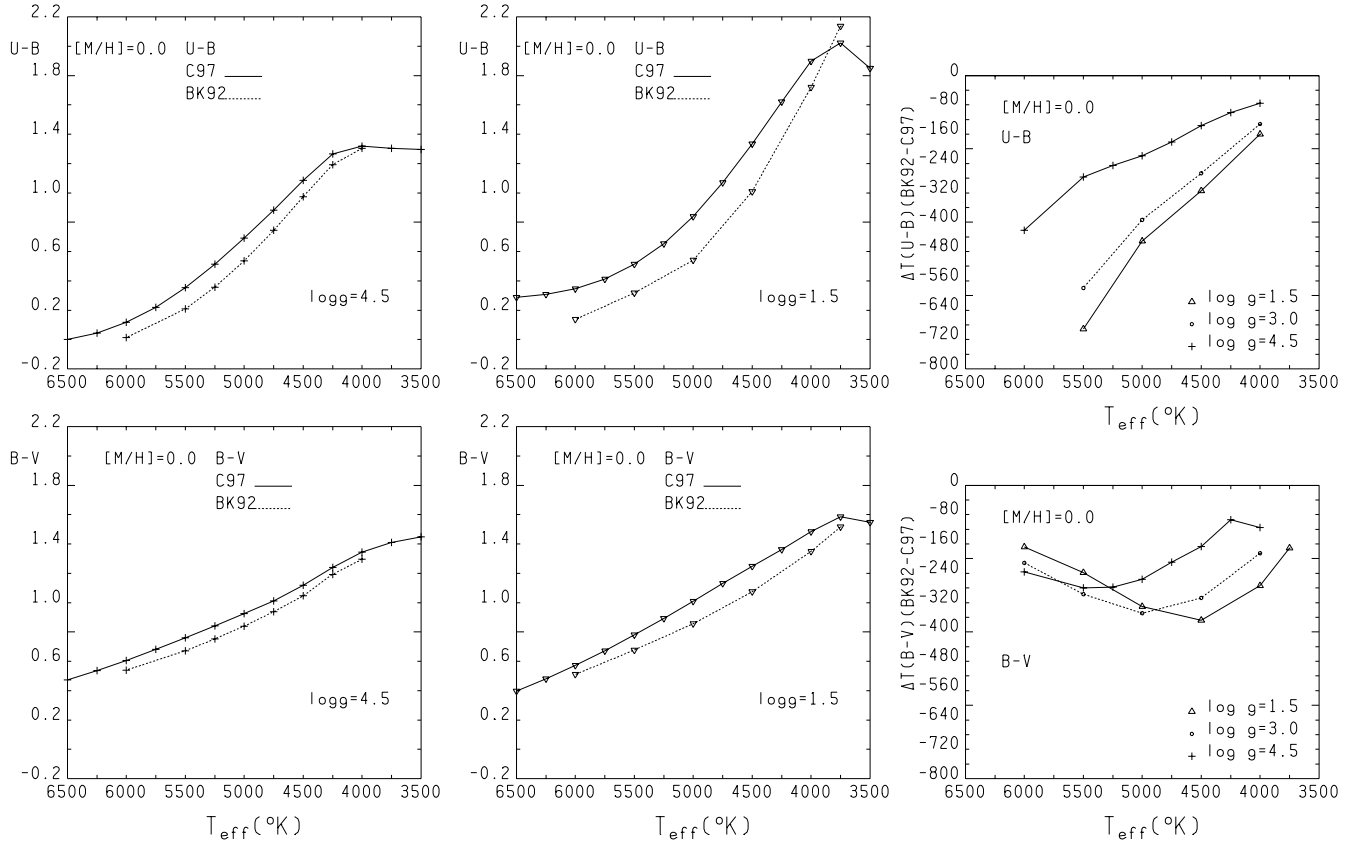


Fig. 10. Comparison between synthetic indices (U-B) and (B-V) from Buser & Kurucz (1992) (dashed line) and from C97 (full line). The plots on the right show the differences between effective temperatures corresponding to the same values of the indices in the two grids

4.5. For instance, we can derive a difference $\Delta T_{eff} = 375$ K for $\log g = 1.5$ and $(U-B) = 0.6$, and $\Delta T_{eff} = 300$ K for $\log g = 1.5$ and $(B-V) = 1.0$.

8. The dependence of the synthetic (U-B), (B-V) colors and bolometric correction on effective temperature, gravity, and metallicity

The computed T_{eff} -color relations show the behaviour of the color indices with temperature, gravity, and metallicity. Fig 11a shows that (U-B) is almost independent of gravity for T_{eff} between 4500 K and 5750 K, and that it strongly depends on T_{eff} in this region. Vice-versa, it depends on $\log g$ for T_{eff} between 6250 K and 8750 K. For $T_{eff} > 9000$ K, (U-B) depends on both T_{eff} and $\log g$. Fig. 11b shows that (U-B) depends on metallicity for $T_{eff} < 8000$ K, while for $T_{eff} > 8000$ K it is almost independent of it.

Fig. 12a shows that (B-V) is almost independent of $\log g$ for T_{eff} between 3750 K and 6250 K. For T_{eff} between 6250 K and 8500 K, (B-V) depends on both T_{eff} and $\log g$; for T_{eff} between 8500 K and 10000 K it still depends on $\log g$ for dwarfs, but it is almost independent of it for $\log g < 4.0$; for $T_{eff} > 11000$ K, (B-V) is almost independent of both T_{eff} and $\log g$. Fig. 12b shows that (B-V) slightly depends on metallicity when it is independent of $\log g$, namely for T_{eff} between 3750 K and 6250 K. For higher T_{eff} , (B-V) is almost independent of metallicity.

The dependence of the color indices on the microturbulent velocity ξ is discussed in Sect. 12 for $[M/H] = -2.0$.

Fig. 13a shows that BC_V is almost independent of $\log g$, in particular for $T_{eff} > 9000$ K. Fig. 13b shows that BC_V slightly depends on metallicity.

Table 2 quantifies, for convective stars, the dependence of (U-B) and (B-V) on metallicity and the dependence of (B-V) on gravity. For the set of T_{eff} given in column 1, column 2 lists, for $\log g = 4.5$, ΔT_{eff} derived at the same (U-B) from the grids computed for $[M/H] = 0.0$ and $[M/H] = -1.0$. For comparison, column 3 lists the corresponding ΔT_{eff} derived from the Alonso et al. (1996b) empirical relations (see Sect. 9). Columns 4 and 5 are the analogous to columns 2 and 3 for $[M/H] = -1.0$ and $[M/H] = -2.0$. Columns 6, 7, 8, and 9 are analogous to columns 2, 3, 4, and 5, but for (B-V). The last two columns show the difference ΔT_{eff} derived at the same (B-V) for $\log g = 3.5$ and $\log g = 4.5$. Column 10 shows the results from the grid computed for $[M/H] = 0.0$ and column 11 is for $[M/H] = -2.0$.

9. Empirical T_{eff} -color relations

Empirical T_{eff} -color relations should be model independent. However, up to now, there are no methods completely independent of models. The most direct method is that proposed by Code et al. (1976), which uses the total observed fluxes and the measured angular diameters. But the observed flux has to

Table 2. Dependence of (U-B) and (B-V) on metallicity and on gravity. See Sect. 8 in the text for the meaning of the columns.

T_{eff} (K)	ΔT_{eff} (K)										
	(U-B)		(U-B)		(B-V)		(B-V)		(B-V)	(B-V)	
	[M/H](0.0,-1.0)	[M/H](-1.0,-2.0)	[M/H](0.0,-1.0)	[M/H](-1.0,-2.0)	[M/H](0.0,-1.0)	[M/H](-1.0,-2.0)	$\log g$ (4.5,3.5)	$\log g$ (4.5,3.5)	[M/H] = 0.0	[M/H] = -2.0	
(1)	(2)	(3)	(4)	(5)	(6)	(7)	(8)	(9)	(10)	(11)	
3500	595		97						409	33	
3750	603		314						68	17	
4000	491		339		133	204:	87	192:	-15	7	
4250	423	458	297	250	222	218:	67	119:	-7	11	
4500	447	509	298	296	273	227	71	131:	-22	23	
4750	486	583	323	321	285	250	101	131	-47	32	
5000	548	680	370	323	287	279	134	132	-46	64	
5250	678	788	465	393	289	286	180	150	-21	97	
5500	1187	1036	5065	458	301	303	202	161	12	115	
5750					323	307	195	161	33	122	
6000					334	340	180	146	57	132	
6250					327	364	154	175	83	151	
6500					311	350	128	182	114	189	
6750					294	406	112	194	145	236	
7000					268	400	97	175:	186	300	
7250					237	500	85		257	366	
7500					206		75		340	453	
7750					162		59		450	544	
8000					111		40		551	655	
8250					81		21		616	750	
8500					83		18		697	819	
8750					67		11		776		

be supplemented with fluxes from models at wavelengths (very long and very short) for which no observations exist to build up the bolometric flux needed to obtain T_{eff} . The extent of the dependence of T_{eff} on models is related to the spectral type of the studied stars. Code et al. (1976) derived T_{eff} for 37 stars with solar metallicity including dwarfs, giants, and supergiants. The quoted accuracy of T_{eff} ranges from 1.4 % to 7.7 %, and, on average, it is on the order of 4 %.

The infrared flux method (IRFM) from Blackwell & Shallics (1977) is also based on the bolometric flux. Furthermore it needs also the computed flux at a some given wavelength in the infrared. This method loses its validity with increasing T_{eff} and cannot be used for $T_{\text{eff}} > 10000$ K. Mégessier (1994) discussed the influence of models on the derivation of T_{eff} . Blackwell & Lynas-Gray (1994) and Blackwell & Lynas-Gray (1998) used this method to analyze both dwarfs and giants, but for only solar or nearly solar metallicity. They estimated the accuracy of T_{eff} they derived with IFRM to be on the order of 2 %.

Also Alonso et al. (1996b) published effective temperatures and T_{eff} -color calibrations based on the infrared flux method. They derived T_{eff} only for dwarfs, but having metallicities ranging from [0.0] to [-2.5]. Relationships θ_{eff-f} -[Fe/H]-color index are given for several indices in the Johnson and Strömgren systems, but not for (U-B). In fact, the particular shape of the T_{eff} -(U-B) curve showing a dependence of (U-B) on T_{eff} for $T_{\text{eff}} < 6000$ K and a dependence of (U-B) on $\log g$ for $T_{\text{eff}} > 6000$ K

(Fig. 11a) can hardly be fitted by some polynomial approximation. The T_{eff} -(U-B) relation in Alonso et al. (1996b) was derived by averaging over the observed (U-B) indices and the corresponding T_{eff} .

The mean accuracy of the adopted metallicity was estimated to be within 0.15 dex and 0.3 dex. From Fig. 11b we see that this uncertainty in metallicity translates into an error in T_{eff} no larger than 150 K near 5000 K and [M/H] = 0.0. The accuracy of T_{eff} was estimated to be on the order of 1.5 % (Alonso et al., 1996a). Finally, for [M/H] = 0.0, the combined uncertainty from the IRFM and metallicity is less than 200 K at 5000 K.

Finally, Gratton et al. (1996) derived empirical T_{eff} -color relations from both dwarfs and giants for [M/H] = 0.0 by using both data from Blackwell & Lynas-Gray (1994) and those from Bell & Gustafsson (1989).

To compare theoretical relations with observations we have used, for cool dwarfs, the Alonso et al. (1996b) T_{eff} -(U-B) and T_{eff} -(B-V) empirical scales, and, for cool giants, the Gratton et al. (1996) T_{eff} -(B-V) empirical calibration. For both dwarfs and giants we added, for comparison, the T_{eff} -color data from Blackwell & Lynas-Gray (1994) (BLG). For dwarfs, the larger number of stars (i.e. 410) used by Alonso et al. (1996b) as compared with the 140 stars used by Gratton et al. (1996) has lead us to give more weight to the Alonso et al. T_{eff} -color relations. Alonso et al. (1996a) assigned to the dwarfs and subdwarfs of their sample a gravity which increases from $\log g = 4.0$ for the

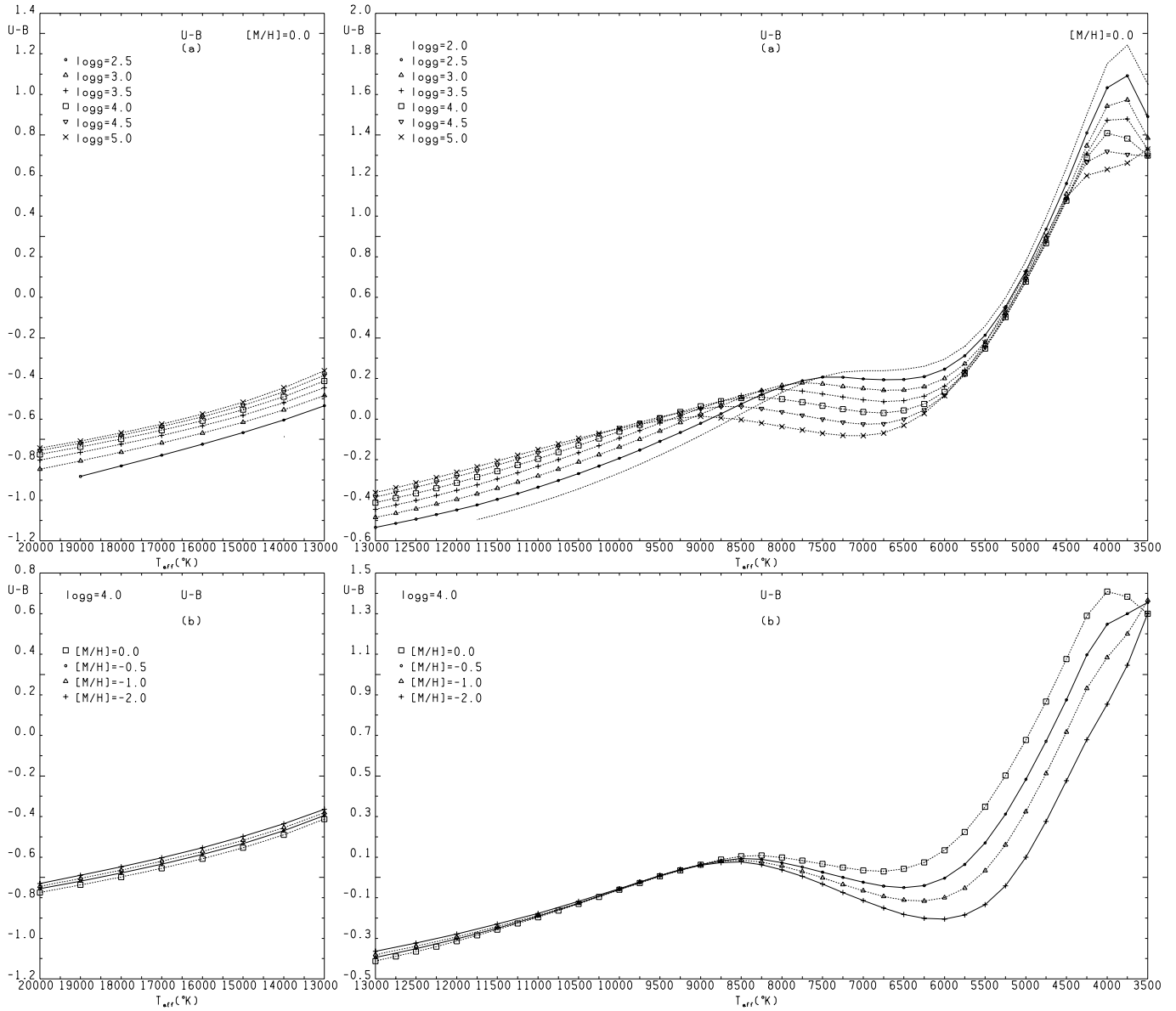


Fig. 11a and b. Computed T_{eff} -(U-B) relations for **a** different $\log g$ and $[M/H] = 0.0$, and **b** for different metallicities and $\log g = 4.0$

hottest Pop I stars to $\log g = 5.0$ for the cooler stars. Gratton et al. (1996) assumed $\log g = 4.5$ for dwarfs; for giants, they assumed $\log g = 2.0$ for $T_{\text{eff}} \geq 4500$ K and $\log g = (T_{\text{eff}} - 3500)/500$ for $T_{\text{eff}} < 4500$ K.

When we used data from BLG we separated dwarfs from giants on the basis of the stellar gravity as listed in Castelli et al. (1997). The gravities of the sample range from $\log g = 1.40$ to $\log g = 4.65$. We assumed that stars with $\log g \geq 3.75$ are dwarfs, while the others are giants. This rough luminosity classification can be compared with the $T_{\text{eff}}-\log g$ relations listed by Gray (1989) which show that $\log g$ for dwarfs increases from 4.2 at 8250 K to 4.7 at 3620 K; $\log g$ for giants decreases from 3.6 at 6380 K to 1.9 at 3880 K. Interpolated values of $\log g$ from Gray (1989) are shown in the last column of Table 3 and Table 4. Bessell et al. (1998) estimated gravities from theoretical isochrones and evolutionary tracks. They pointed out that

“gravities of stars on the solar abundance giant branch range from $\log g = 3.0 \pm 0.5$ near 5000 K to $\log g = -0.2 \pm 0.5$ at 3000 K”.

We dereddened the stars of the BLG sample by using the relations taken from Schmidt-Kaler (1992):

$$E(B - V) = A(V)/3.12 \quad (11)$$

$$E(U - B) = 0.72E(B - V) + 0.05E(B - V)^2 \quad (12)$$

For both hot dwarfs and hot giants we considered the empirical T_{eff} -(U-B) data and empirical T_{eff} -(B-V) calibration from Code et al. (1976). We adopted the $T_{\text{eff}}-\log g$ calibrations from Schmidt-Kaler (1982). Namely, for main sequence stars, $\log g$ is about 4.0, while for giants it is on the order of 3.5. For the giants and dwarfs listed in Code et al. (1976) we adopted (U-B) taken from the Bright Star Catalog (Warren & Hoffleit, 1994) and we dereddened them with the relations (11) and (12).

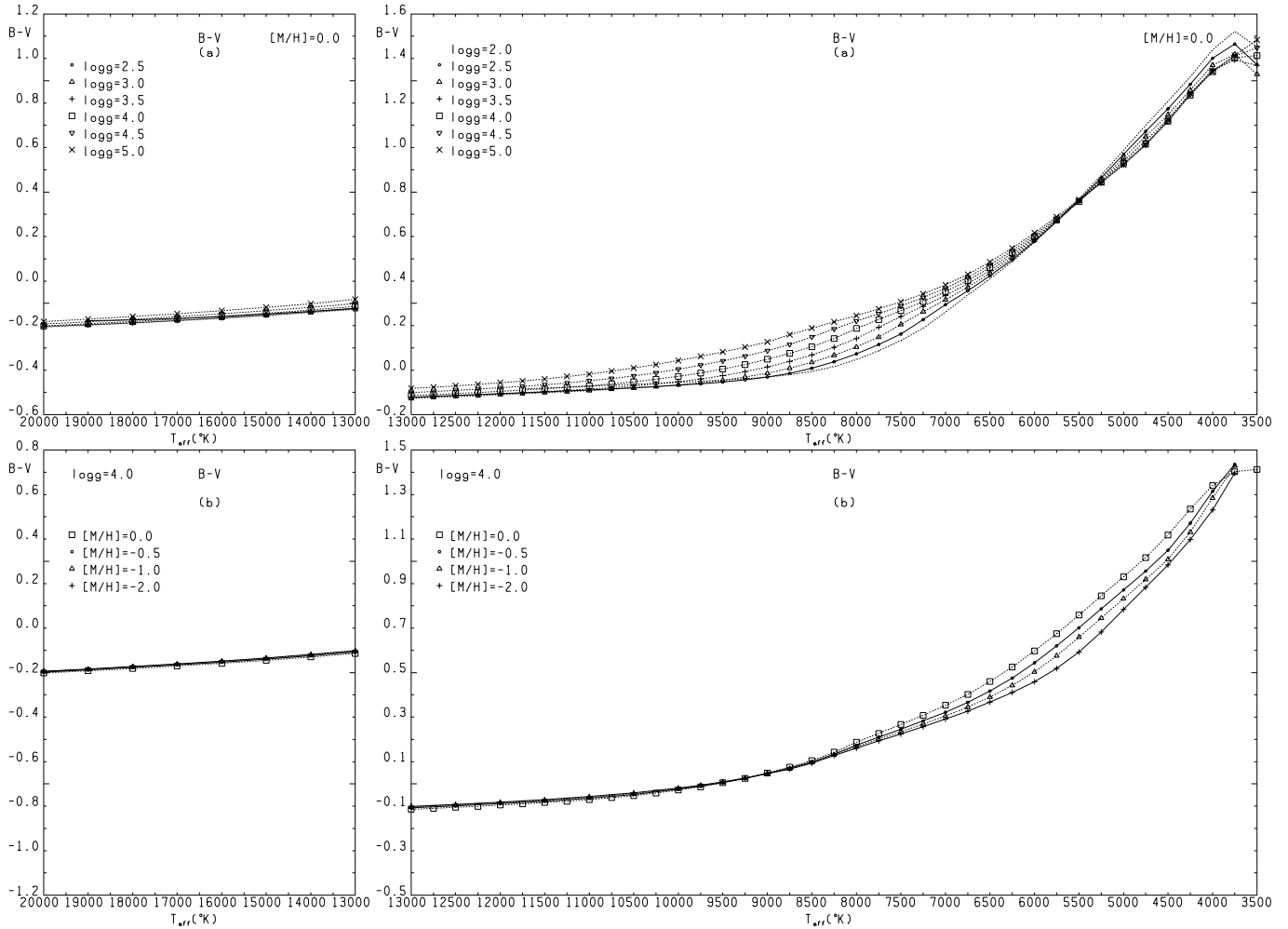


Fig. 12a and b. Computed T_{eff} -(B-V) relations for **a** different $\log g$ and $[M/H] = 0.0$, and **b** for different metallicities and $\log g = 4.0$

9.1. Comparison of empirical T_{eff} -color relations for cool stars

Fig. 14 compares the T_{eff} -(U-B) and T_{eff} -(B-V) empirical relations from Alonso et al. (1996b) (full line) with the T_{eff} -(U-B) and T_{eff} -(B-V) color data taken from the BLG sample for dwarfs (asterisks). The empirical relation T_{eff} -(B-V) from Gratton et al. (1996) is also plotted (dashed lines). The Alonso et al. (1996b) empirical relations are slightly redder than both Gratton et al. (1996) and BLG T_{eff} -color data.

This small discrepancy between the different empirical relations could be related with the different photometric observations adopted by the different authors. For instance, Alonso et al. (1996b) use UBV data mostly from Sandage & Kowall (1986) and Carney & Latham (1987). Ryan (1989) presented much accurate and original UBV photometry for subdwarfs and states that his (U-B) photometry is in agreement with Sandage & Kowall (1986), but that the Carney & Latham (1987) U-B photometry is about 0.02 mags redder. As consequence, the Alonso et al. (1996b) T_{eff} -(U-B) empirical relations could be shifted toward the blue if Ryan (1989) observations are used.

10. Comparison of computed and empirical T_{eff} -color relations

To compare the empirical T_{eff} -color relations with the computed ones we should pick out the atmospheric models having parameters T_{eff} and $\log g$ as close as possible to those of the stars used to build up the empirical relations. For cool stars ($T_{\text{eff}} < 9000$ K) we estimated the T_{eff} - $\log g$ dependence from Gray (1989) and from the isochrones of Bertelli et al. (1994).

Table 3 and Table 4 show, for dwarfs and giants respectively, the T_{eff} - $\log g$ dependence for stars with $[M/H] = 0.0$, when the isochrones for metallicity $Z = 0.02$ and $\log(\text{age})$ equal to 9.6 and 9.0 yr are considered. For comparison, the last column lists the T_{eff} - $\log g$ calibration from Gray (1989).

Because, according to Bessell et al. (1998), the uncertainty in gravity derived from the isochrones is on the order of ± 0.5 dex, we averaged and smoothed the $\log g$ - T_{eff} relations of Table 3 and Table 4. Without going beyond the uncertainty limits of ± 0.5 dex for $\log g$, we recovered the same parameters available in the grids of models. We recall that the steps $\Delta \log g$ are equal to 0.5 dex in the K95 and C97 grids. For dwarfs, we adopted $\log g = 4.5$ for $T_{\text{eff}} \leq 6500$ K, and $\log g = 4.0$ for the

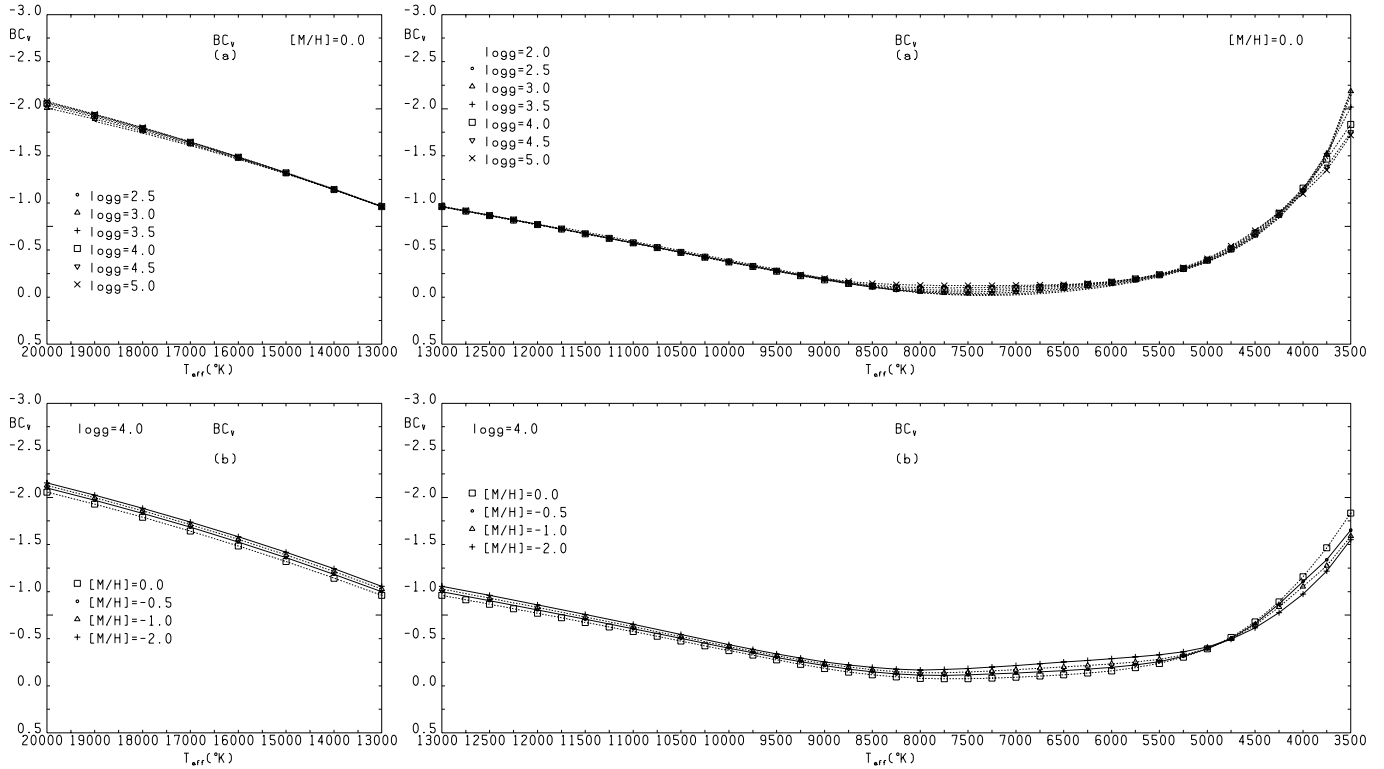


Fig. 13a and b. Computed $T_{\text{eff}}-BC_V$ relations for **a** different $\log g$ and $[M/H]=0.0$, and **b** for different metallicities and $\log g=4.0$

Table 3. $\log g-T_{\text{eff}}$ calibrations for dwarfs derived both from the Bertelli et al. (1994) isochrones of different ages and $Z=0.02$ and from Gray (1989)

T_{eff}	isochrones		Gray (1989)
	9.6	9.0	$\log g$
	$\log g$	$\log g$	
8000			4.22
7750			4.22
7500			4.23
7250		4.13	4.24
7000		4.20	4.25
6750		4.26	4.25
6500		4.32	4.27
6250		4.39	4.28
6000	4.38	4.46	4.31
5750	4.47	4.52	4.36
5500	4.52	4.56	4.44
5250	4.57	4.59	4.49
5000	4.60	4.62	4.51
4750	4.63	4.63	4.53
4500	4.65	4.67	4.54
4250	4.68	4.70	4.57
4000	4.72	4.71	4.60

hotter stars. For giants, we adopted:

$\log g = 3.5$ for $T_{\text{eff}} \geq 5500$ K
 $\log g = 3.0$ for $4750 \text{ K} \leq T_{\text{eff}} < 5500$ K

Table 4. $\log g-T_{\text{eff}}$ calibrations for giants derived both from the Bertelli et al. (1994) isochrones of different ages and $Z=0.02$ and from Gray (1989)

T_{eff}	isochrones		Gray (1989)
	9.6	9.0	$\log g$
	$\log g$	$\log g$	
7250			3.62
7000			3.55
6750			3.47
6500			3.42
6250			3.36
6000	3.90	3.32	3.6
5750	3.83	3.30	3.5
5500	3.79	3.29	3.4
5250	3.76	3.29	3.3
5000	3.68	3.17	3.2
4750	3.10	2.71	3.1
4500	2.50	2.23	2.7
4250	1.99	1.78	2.5
4000	1.50	1.26	2.2

$\log g = 2.5$ for $4500 \text{ K} \leq T_{\text{eff}} < 4750$ K

$\log g = 2.0$ for $4250 \text{ K} \leq T_{\text{eff}} < 4500$ K

$\log g = 1.5$ for $4000 \text{ K} \leq T_{\text{eff}} < 4250$ K

For hot dwarfs and giants, ($T_{\text{eff}} \geq 9000$ K) we adopted models with $\log g = 4.0$, and $\log g = 3.5$ respectively, in accordance with

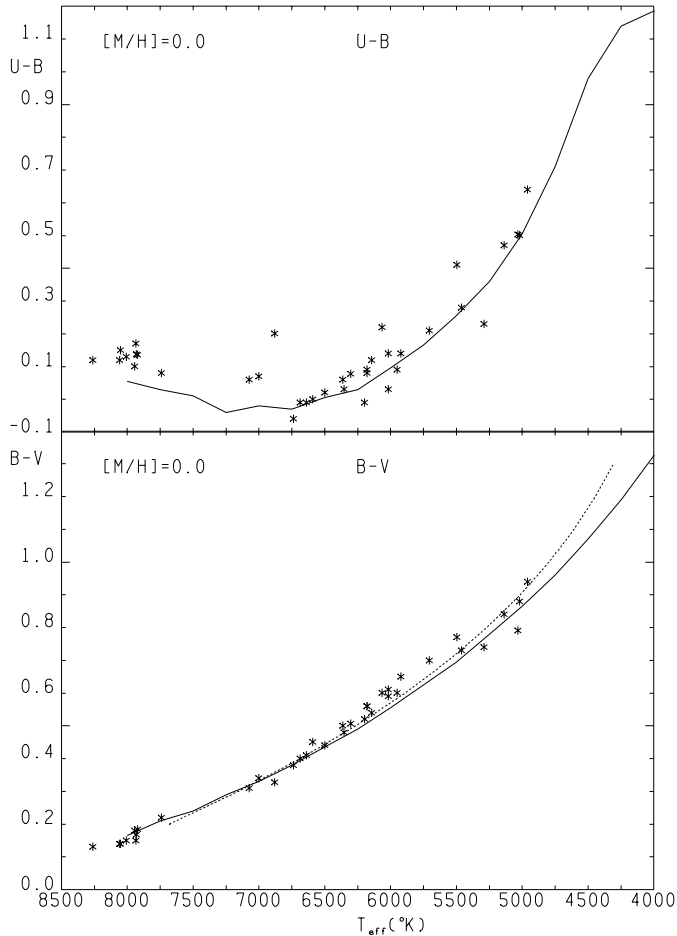


Fig. 14. Comparison of the Alonso et al. (1966b) T_{eff} -(U-B) and T_{eff} -(B-V) empirical relations for $[M/H] = 0.0$ (full lines) with the data for dwarfs taken from the BLG sample (asterisks). For (B-V), the Gratton et al. (1996) empirical relation for dwarfs is also considered (dashed line)

the spectral type- T_{eff} relations and spectral type- $\log g$ relations from Schmidt-Kaler (1982).

Because, in the BK92 grids, the gravities of the models may be different from those of the K95 and C97 grids, we have changed a little bit the $\log g$ - T_{eff} relation when we compared observations with the BK92 colors. The adopted $\log g$ are shown in Fig. 16 and Fig. 19. They do not differ more than ± 0.5 dex from the gravities adopted with the C97 and K95 grids.

10.1. T_{eff} -(U-B) relations

10.1.1. $3500 \text{ K} < T_{\text{eff}} < 9000 \text{ K}$

Fig. 15a compares, for dwarfs, theoretical relations T_{eff} -(U-B) from C97 for $[M/H] = 0.0$ with the corresponding empirical relations from Alonso et al. (1996b) and with the T_{eff} -color data taken from the BLG sample for dwarfs. Fig. 15c is the same comparison for giants. In this case the data (the asterisks) are only those from BLG.

For dwarfs, models give higher T_{eff} than the Alonso et al. (1996b) empirical relation when the (U-B) index depends on T_{eff} , namely for T_{eff} lower than about 6000 K. For $T_{\text{eff}} > 6000 \text{ K}$ the Alonso et al. (1996b) empirical relation would agree with a relation computed for $\log g = 4.5$ rather than with the one for $\log g = 4.0$. The theoretical T_{eff} -color relation fits better the BLG data than the empirical relation from Alonso et al. (1996b).

The discrepancy between the computed T_{eff} -(U-B) relations and the Alonso et al. empirical relations does not change in a significant way with the metallicity. Fig. 15b shows the ΔT_{eff} differences as a function of T_{eff} for $\log g = 4.5$ and $[M/H] = 0.0, -1.0, \text{ and } -2.0$ when the same (U-B) is considered in Alonso et al. (1966b) empirical relations and in the computed relations. For $[M/H] = 0.0$ and $\log g = 4.5$, the largest difference is $\Delta T_{\text{eff}} = 265 \text{ K}$ at 5000 K. This discrepancy is larger than the estimated uncertainty of 200 K in T_{eff} related with the IRFM method (Sect. 9).

We may deduce from Fig. 3 that the K95 models do not improve the situation. Furthermore, for dwarfs and $T_{\text{eff}} > 5500 \text{ K}$, they would fit the empirical relation for a gravity larger than 4.5 dex. Fig. 6 indicates that the discrepancy slightly decreases with the BCP colors.

Fig. 15c shows a rather good agreement for giants between the T_{eff} -(U-B) data from the BLG sample and the relation from models with parameters fixed by the adopted $\log g$ - T_{eff} calibration.

Fig. 16 shows that, instead, the Buser & Kurucz (1992) (BK92) synthetic colors give good agreement with the observations for dwarfs and T_{eff} between 4000 K and 5500 K, while they give cooler T_{eff} than the observations for giants. We checked that this behaviour does not change for lower metallicities.

10.1.2. $T_{\text{eff}} \geq 9000 \text{ K}$

Fig. 17 compares computed T_{eff} -(U-B) relations for $[M/H] = 0.0$ and $\log g$ equal to 4.0 and 3.5 with T_{eff} -(U-B) values for the dwarfs and giants analyzed by Code et al. (1976). The computed relations agree with the observed T_{eff} -(U-B) within the error limits and the theoretical curves follow the behaviour of the observed points. The error bars on the observed points show that the uncertainty in the observed T_{eff} increases with increasing T_{eff} .

10.2. T_{eff} -(B-V) relations

10.2.1. $3500 \text{ K} < T_{\text{eff}} < 9000 \text{ K}$

Fig. 18a and Fig. 18c compare theoretical relations T_{eff} -(B-V) from C97 for $[M/H] = 0.0$ with the corresponding empirical relations from Alonso et al. (1996b) for dwarfs, and from Gratton et al. (1996) for giants, respectively. The T_{eff} -color data obtained from the BLG sample for both dwarfs and giants are also given for comparison.

Models give higher T_{eff} than the empirical relations for both dwarfs and giants. Fig. 18b shows, for dwarfs, the ΔT_{eff} differences as a function of T_{eff} for the same (B-V) in Alonso et

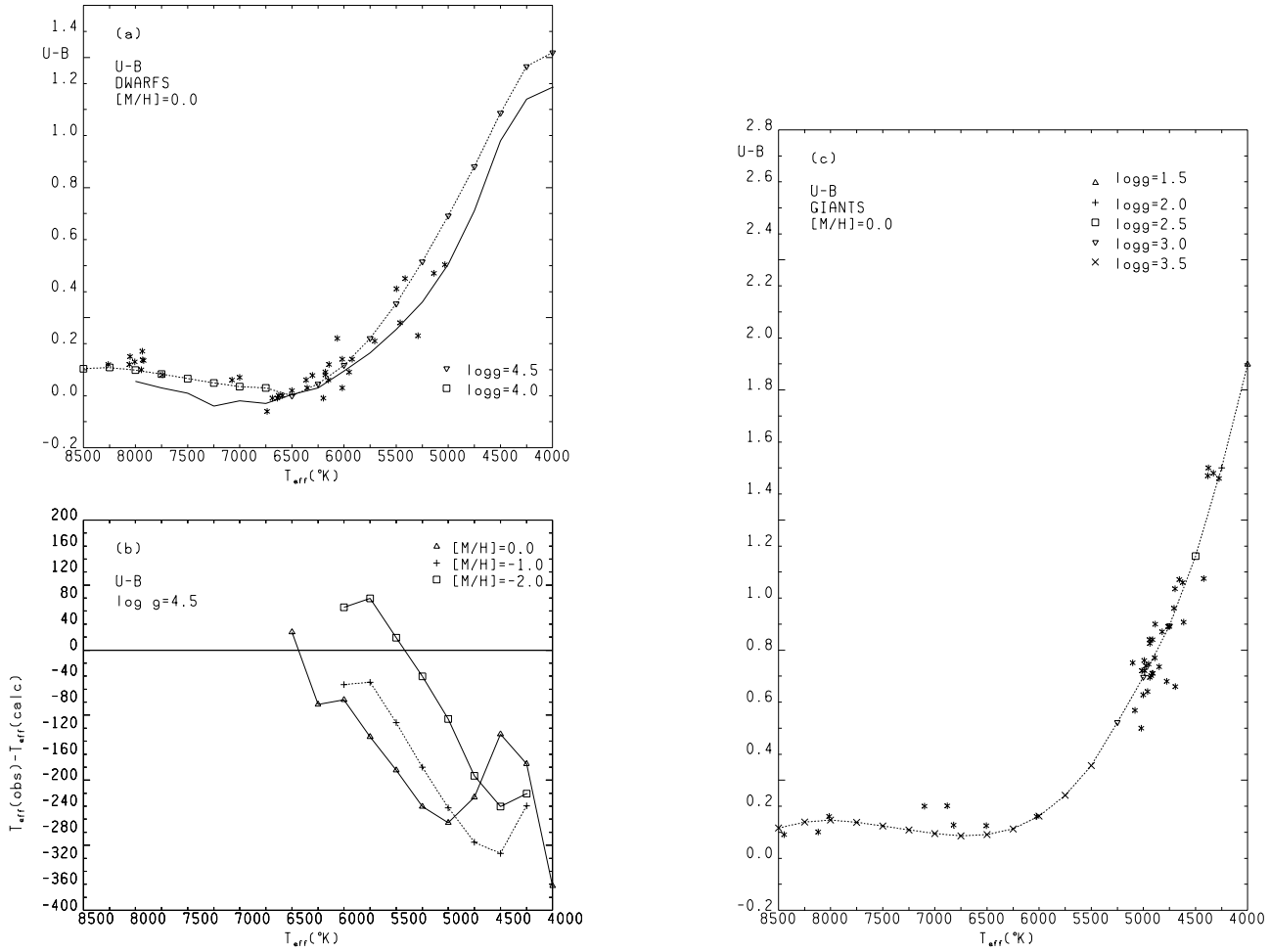


Fig. 15. **a** and **c**: The empirical relations $T_{\text{eff}}(\text{U-B})$ from Alonso et al. (1996b) (full line) and the data from the BLG sample (asterisks) are compared with the theoretical relations from C97 for $[M/H] = 0.0$ (dashed line) **b** ΔT_{eff} differences from Alonso et al. (1996b) empirical relations for $[M/H] = 0.0, -1.0$, and -2.0 and the corresponding computed relations for $\log g = 4.5$

al. (1966b) and in the computed $T_{\text{eff}}(\text{B-V})$ relations. ΔT_{eff} is plotted for the different metallicities $[M/H] = 0.0, -1.0$, and -2.0 . The agreement between the theoretical $T_{\text{eff}}(\text{B-V})$ relation and the Alonso et al. empirical relations does not change with the metallicity in a significant way for $T_{\text{eff}} < 6000$ K. For $T_{\text{eff}} > 6000$ K, ΔT_{eff} increases with decreasing metallicity. For $[M/H] = 0.0$, the maximum ΔT_{eff} is 200 K at 5500 K. This discrepancy is of the same order as the 200 K uncertainty associated with the IRFM method.

Also for giants, for $[M/H] = 0.0$, the differences between the empirical and theoretical $T_{\text{eff}}(\text{B-V})$ relations lie within the uncertainty limit of 200 K in T_{eff} .

From Fig. 4 we may deduce that the disagreement between the empirical and the computed $T_{\text{eff}}(\text{B-V})$ relations increases when the K95 colors are used, while Fig. 7 indicates that the discrepancy does not change in a significant way when the BCP colors are used.

Fig. 19 shows that, for dwarfs, the BK92 synthetic colors gives slightly cooler T_{eff} than those from observations. ΔT_{eff} is about 60 K. For giants, the BK92 indices give ΔT_{eff} larger than those from the new grids of colors.

Further comparisons for (B-V) and BK92 are presented by Alonso et al. (1996b).

10.2.2. $T_{\text{eff}} \geq 9000$ K

Fig. 20a compares the empirical $T_{\text{eff}}(\text{B-V})$ relation from Code et al. (1976) for dwarfs and giants with the corresponding relations from models.

Fig. 20b shows the ΔT_{eff} differences as a function of T_{eff} for $\log g = 4.0$ when the same (B-V) is considered in the empirical and computed relations. Full line and dashed lines are for indices normalized to $(\text{B-V}) = -0.016$ (Hayes, 1985) and $(\text{B-V}) = 0.000$ (Johnson et al., 1966) for Vega, respectively. The increasing difference ΔT_{eff} with increasing T_{eff} is related to the decreasing sensitivity of (B-V) with temperature, as can be inferred from the slope of the $T_{\text{eff}}(\text{B-V})$ curve drawn in Fig. 20a. The agreement between the observed and computed $T_{\text{eff}}(\text{B-V})$ relations is better when $(\text{B-V})_{\text{Vega}} = -0.016$ is adopted as the zero-point. These comparisons point out the importance of high accuracy for the observed indices of some standard stars, in order to be able to fix the zero-points of the synthetic colors.

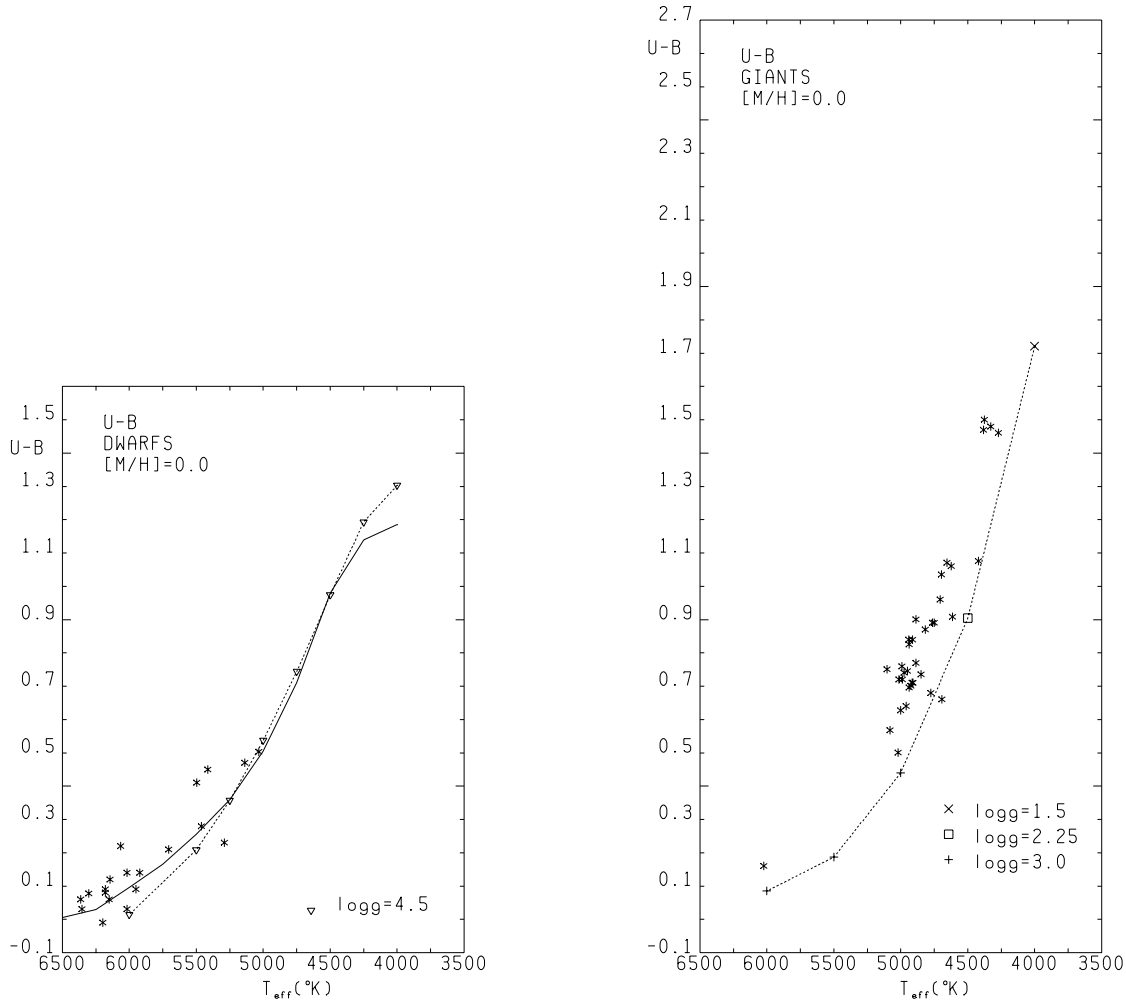


Fig. 16. Buser & Kurucz (1992) T_{eff} -(U-B) relations (dashed line) are compared with the empirical relation from Alonso et al. (1996b) (full line) and with the BLG data (asterisks)

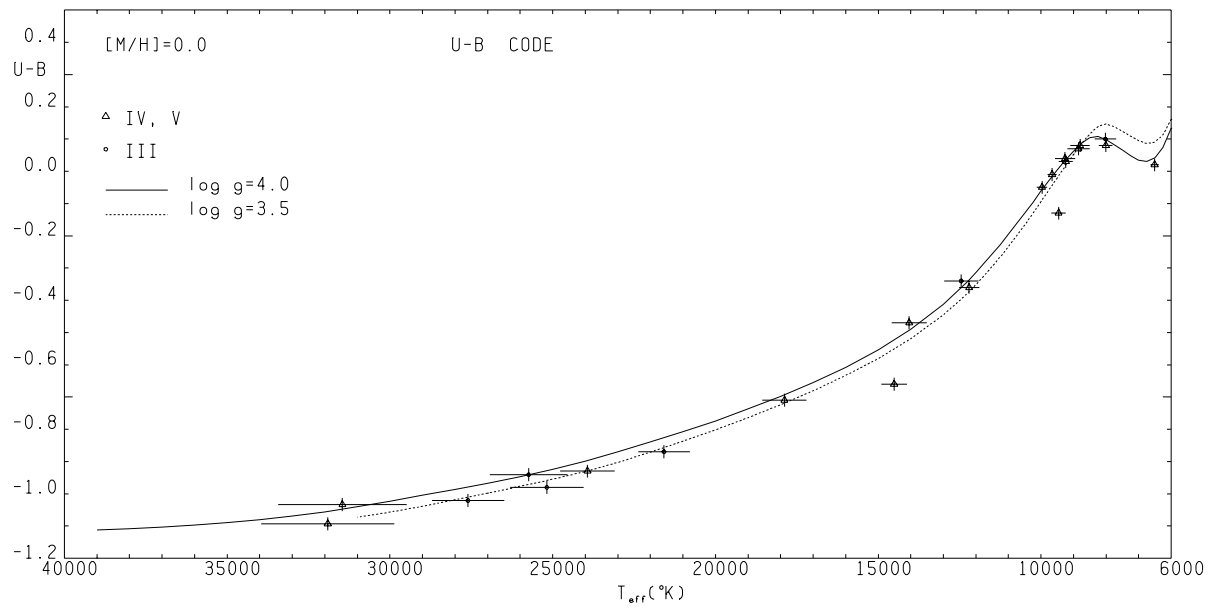


Fig. 17. (U-B) index versus empirical T_{eff} from Code et al. (1976) for dwarfs (triangles) and giants (points) is compared with the T_{eff} -(U-B) theoretical relations from K95 for $\log g = 4.0$ (full line) and $\log g = 3.5$ (dashed line)

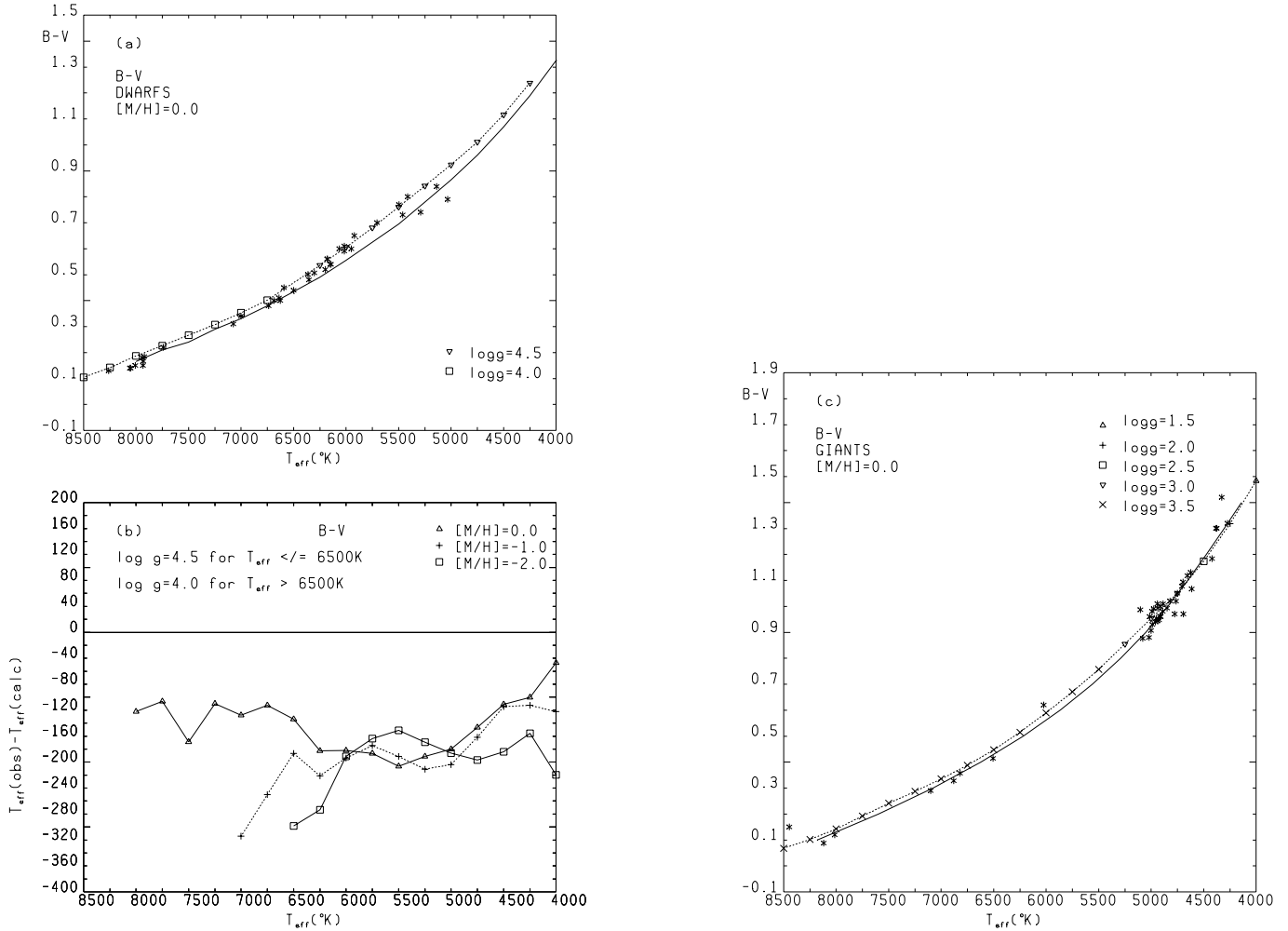


Fig. 18. (a),(c):The empirical relations $T_{\text{eff}}(\text{B-V})$ from Alonso et al. (1996b) for dwarfs (full line) and from Gratton et al. (1996) for giants (full line) and the data from the BLG sample (asterisks) are compared with the theoretical relations from C97 for $[\text{M}/\text{H}] = 0.0$ (dashed line). (b) ΔT_{eff} differences from Alonso et al. (1996b) empirical relations for $[\text{M}/\text{H}] = 0.0, -1.0,$ and -2.0 and the corresponding computed relations for $\log g = 4.5$

The (B-V) indices from BCP have the same behaviour as the C97 or K95 indices, as is also evident from Fig. 9.

11. Computed and empirical T_{eff} -bolometric correction relations

We compared the computed T_{eff} -bolometric correction BC_V relation for $[\text{M}/\text{H}] = 0.0$ with the empirical $T_{\text{eff}}\text{-BC}_V$ relation for dwarfs and giants taken from Code et al. (1976). T_{eff} ranges from 5780 K to 34000 K. The errors of the empirical BC_V range from 0.04 mag to 0.23 mag and they increase with increasing T_{eff} .

The comparison of the computed BC_V with the observed ones requires the same zero-point for both. Therefore to compare BC_V from K95 or C97 with empirical BC_V from Code et al. (1976), the zero-point has to be shifted to $\text{BC}_{V\odot} = -0.07$, the value assumed by Code et al. (1976) for $\text{BC}_{V\odot}$. Fig. 21 compares the bolometric corrections BC'_V (which is the computed BC_V renormalized to $\text{BC}_{V\odot} = -0.07$) for $\log g = 4.0, 4.5,$ and

5.0 with the empirical bolometric corrections from Code et al. (1976). The results are the same for the C97 or K95 and BCP colors, because the computed BC_V do not change in the different synthetic grids. The agreement is of the same quality as that shown in Fig. 7 of the Buser & Kurucz (1978) paper.

12. The new models and the effect of abundance and microturbulent velocity on colors

Fig. 22 shows the differences in the computed T_{eff} -color relations when models with different abundances for iron and for the α elements are used. The two cases for $\log g = 4.5$ and $\log g = 1.5$ are considered. As expected, the indices differ when they depend on metallicity, in particular for $T_{\text{eff}} < 5000$ K. For $\log g = 4.5$, we compared the computed relations with the empirical relations from Alonso et al. (1996b). The models for $[\text{M}/\text{H}] = -2.0$ give an excellent agreement between observed and empirical relations, removing the discrepancy discussed in Sect. 10 and shown in Fig. 15 and Fig. 18.

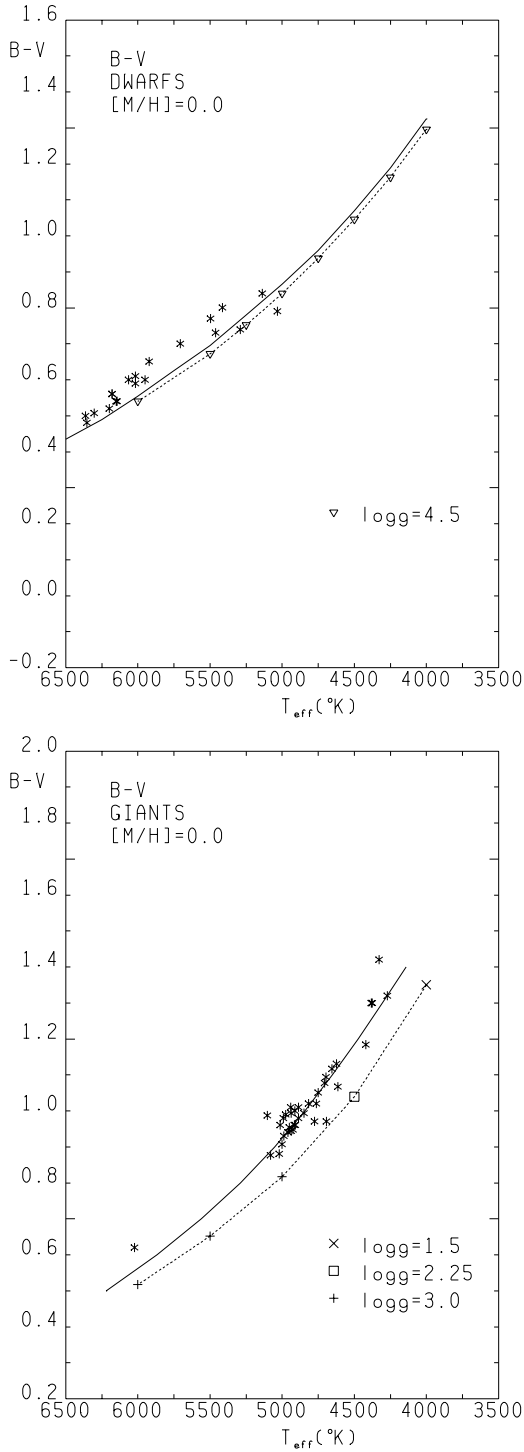


Fig. 19. Buser & Kurucz (1992) T_{eff} -(B-V) relations (dashed line) are compared with the empirical relations from Alonso et al. (1996b) for dwarfs (full line) and Gratton et al. (1996) for giants (full line) and with the BLG data (asterisks)

Fig. 23 shows the differences in the computed T_{eff} -color relations when models with different microturbulent velocities ξ are used. The two cases for $\log g = 4.5$ and $\log g = 1.5$ are considered. The effect is more important for (U-B) than for (B-V), and

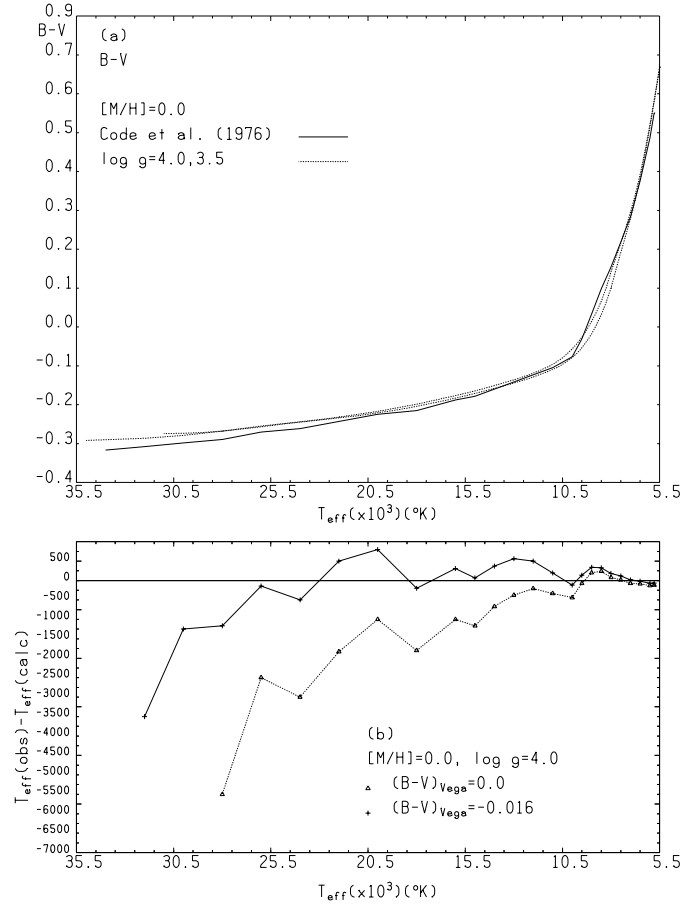


Fig. 20. (a) Comparison of (B-V)- T_{eff} empirical relations from Code et al. (1976) (full line) with C97 (\sim K95) theoretical relations for $[M/H] = 0.0$ and $\log g = 4.0, 3.5$ (dashed lines from top to bottom). (b) ΔT_{eff} as a function of T_{eff} for $\log g = 4.0$ for the same value of the (B-V) index in the computed and empirical T_{eff} -(B-V) relation. The two lines correspond to two different normalization of the (B-V) index. Upper line and lower line correspond to (B-V) = -0.16 and (B-V) = 0.0 for Vega, respectively

increases with decreasing gravity. If the (U-B) or (B-V) index depends on T_{eff} , T_{eff} decreases with decreasing ξ , for a given value of the index. Namely T_{eff} decreases with decreasing line-blanketing. For $\log g = 4.5$, we also plotted in Fig. 23 the T_{eff} -color empirical relations from Alonso et al. (1996b)(asterisks).

13. The Sun

Table 5 lists the observed (U-B) and (B-V) indices for the Sun together with the computed indices in the different grids. Solar models have parameters $T_{\text{eff}} = 5770$ K, $\log g = 4.4377$, $\xi = 1.5$ km s $^{-1}$.

Although the BK92 grid seems to better reproduce the observed indices of dwarfs than the successive grids do, the solar (U-B) and (B-V) indices from BK92 are from 0.05 mag to 0.1 mag lower than the observed ones. The K95 and C97 grids better reproduce (U-B) than the BCP grid, while all three grids K95, C97, and BCP give approximately the same (B-V) for the

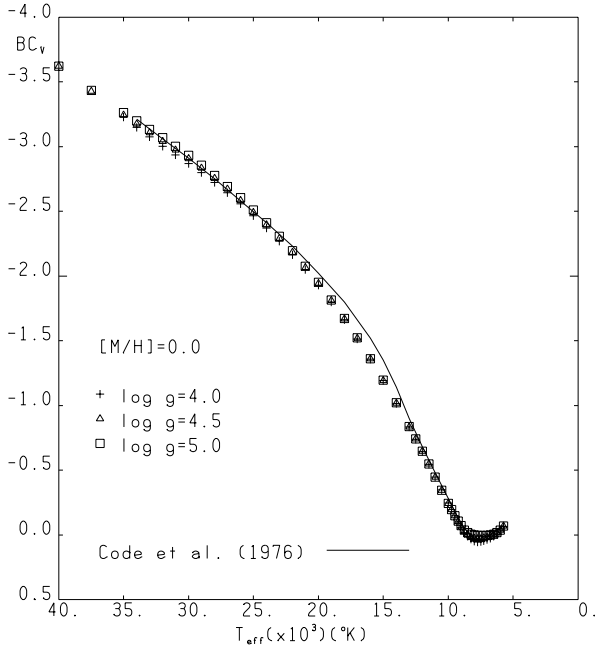


Fig. 21. Comparison of $BC_V - T_{\text{eff}}$ empirical relation from Code et al. (1976) (full line) with computed relations (symbols)

Table 5. Observed and computed color indices for the Sun

Color	Observed	K95	C97	BCP	BK92
$(U - B)$	0.195 ¹ 0.17±0.01 ² 0.183±0.020 ⁴	0.17	0.186	0.145	0.082
$(B - V)$	0.650 ¹ 0.68±0.005 ² 0.648±0.005 ³ 0.686±0.011 ⁴ 0.642±0.004 ⁵	0.67	0.663	0.667	0.593

¹ Neckel (1994), ² Schmidt-Kaler (1982), ³ Gray (1995)

⁴ Tüg & Schmidt-Kaler (1982), ⁵ Cayrel de Strobel (1996)

Sun. The computed $(B-V)$ indices are about 0.02 mag higher than the last determination $(B-V)_{\odot} = 0.642 \pm 0.004$ (Cayrel de Strobel, 1996). This difference corresponds to $\Delta T_{\text{eff}} \sim 80$ K.

We point out the larger difference derived from the computed and empirical $T_{\text{eff}} - (B-V)$ relations at $T_{\text{eff}} = 5750$ K, $\log g = 4.50$. In this case, ΔT_{eff} is on the order of 200 K.

14. Conclusions

The comparison of the synthetic $(U-B)$ and $(B-V)$ indices from the different grids has shown that, in convective stars, the indices are affected both by the treatment of convection and by the amount of line blanketing induced by abundances and microturbulent velocities. In contrast, the bolometric correction BC_V is almost the same in all the grids. When the atmospheric models are the same, the differences resulting from the passbands and zero-points adopted by Kurucz (1995) and Bessell et al. (1998)

Table 6. ΔT_{eff} between Alonso et al. (A) (1996b) empirical relations and the computed grids at $T_{\text{eff}} = 5000$ K, $\log g = 4.5$, $[M/H] = 0.0$ (column 3) and at $T_{\text{eff}} = 7000$ K, $\log g = 4.0$, $[M/H] = 0.0$ (column 4)

		$(T_{\text{eff}}(\text{K}), \log g, [M/H])$	
		$(5000, 4.5, 0.0)$	$(7000, 4.0, 0.0)$
		$\Delta T_{\text{eff}}(\text{K})$	$\Delta T_{\text{eff}}(\text{K})$
$(U - B)$	$T_{\text{eff}}(\text{A}) - T_{\text{eff}}(\text{C97})$	-265	
	$T_{\text{eff}}(\text{A}) - T_{\text{eff}}(\text{K95})$	-251	
	$T_{\text{eff}}(\text{A}) - T_{\text{eff}}(\text{BCP})$	-180	
	$T_{\text{eff}}(\text{A}) - T_{\text{eff}}(\text{BK92})$	0	
$(B - V)$	$T_{\text{eff}}(\text{A}) - T_{\text{eff}}(\text{C97})$	-180	-127
	$T_{\text{eff}}(\text{A}) - T_{\text{eff}}(\text{K95})$	-190	-206
	$T_{\text{eff}}(\text{A}) - T_{\text{eff}}(\text{BCP})$	-196	-111
	$T_{\text{eff}}(\text{A}) - T_{\text{eff}}(\text{BK92})$	+60	

are very small. Some non negligible difference for $(U-B)$ between the BCP and the other two grids K95 and C97 are mostly related to the scaling factor applied by BCP to the computed $(U-B)$ indices.

For dwarfs, the $(U-B)$ and $(B-V)$ indices in all the K95, C97, and BCP grids always give larger T_{eff} than the Alonso et al. (1996b) empirical relations, for all the three metallicities examined $[M/H] = 0.0, -1.0, \text{ or } -2.0$. The largest discrepancies range from 200 K to 300 K and depend on T_{eff} in a different way in each grid. Table 6 lists these discrepancies for $[M/H] = 0.0$ at $T_{\text{eff}} = 5000$ K, $\log g = 4.5$ and $T_{\text{eff}} = 7000$ K, $\log g = 4.0$.

In general, it is very difficult to state which grid reproduces the empirical relations best, owing to the very small differences between the synthetic grids and owing to the uncertainties in the empirical relations. The BCP grid seems slightly superior to the K95 and C97 grids. The BK92 grid well fits the $T_{\text{eff}} - (U-B)$ and $T_{\text{eff}} - (B-V)$ relations for dwarfs, but gives too low temperatures for giants. For the Sun, both the K95 and C97 computed colors reproduce the observed colors better than the BK92 and the BCP colors do.

The improved agreement between empirical and computed $T_{\text{eff}} - \text{color}$ relations for metal-poor dwarfs when models with more realistic abundances for these stars are used (α elements enhanced, new Fe abundance), has led us to plan to extend the grids of models to more abundances and microturbulent velocities in order to cover the H-R diagram as closely as possible.

We finally remark that neither $(U-B)$ nor $(B-V)$ are good indices with which to derive stellar atmosphere parameters. In fact, when $(U-B)$ depends only on T_{eff} ($T_{\text{eff}} \sim 4250 - 5750$ K) or only on $\log g$ ($T_{\text{eff}} \sim 5750 - 7500$ K) it strongly depends on metallicity. When $(U-B)$ weakly depends on metallicity ($T_{\text{eff}} > 9000$ K), it depends on both T_{eff} and $\log g$.

When $(B-V)$ depends on T_{eff} and not on gravity ($T_{\text{eff}} \sim 4000 - 6750$ K), it depends on metallicity (even if to a lesser extent than does the $(U-B)$ index), then when it does not depend on metallicity it depends on both T_{eff} and $\log g$ ($6750 \text{ K} < T_{\text{eff}} < 11000$ K), and finally it is almost independent of both T_{eff} and $\log g$ ($T_{\text{eff}} > 11000$ K).

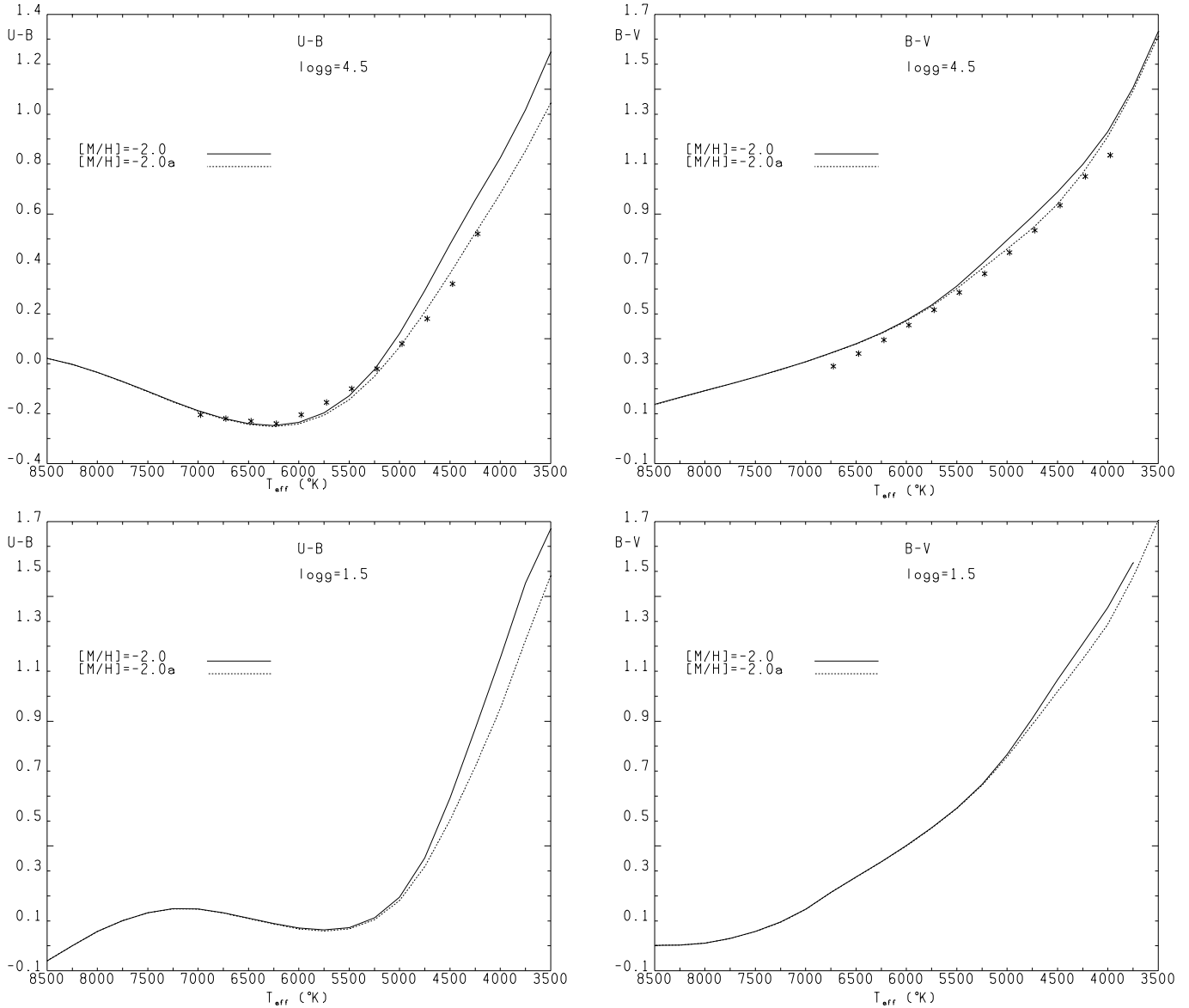


Fig. 22. Computed $T_{\text{eff}}(U-B)$ and $T_{\text{eff}}(B-V)$ relations from models with $[M/H] = -2.0$ (full lines) and $[M/H] = -2.0a$ (dashed lines). The empirical relations from Alonso et al. (1996b) (asterisks) are compared with the relations computed for $\log g = 4.5$. Upper plots are for $\log g = 4.5$, lower plots are for $\log g = 1.5$

Only for B1-B8 stars the $(U-B)$ and $(B-V)$ indices are well suited to derive T_{eff} , provided that they are combined into the Q index, where $Q = (U-B) - 0.72(B-V)$ (Schmidt-Kaler, 1982).

Acknowledgements. The author thanks Robert Kurucz for useful discussions and suggestions and the referee Michael Bessell for his helpful comments.

References

- Alonso A., Arribas S., Martinez-Roger C., 1996a, *A&AS* 117, 227
 Alonso A., Arribas S., Martinez-Roger C., 1996b, *A&A* 313, 873
 Anders E., Grevesse N., 1989, *Geochim. Cosmochim. Acta* 53, 197
 Anstee S.D., O'Mara B.J., 1995, *MNRAS* 276, 859
 Anstee S.D., O'Mara B.J., Ross J.E., 1997, *MNRAS* 284, 202
 Azusienis A., Straizys V., 1969, *Soviet Astron. AJ* 13, 316
 Bell R.A., Eriksson K., Gustafsson B., Nordlund A., 1976, *A&AS* 23,37
 Bell R.A., Gustafsson B., 1989, *MNRAS* 236, 653
 Bertelli G., Bressan A., Chiosi C., Fagotto F., Nasi E., 1994, *A&AS* 106, 275
 Bessell M.S., 1983, *PASP* 95, 480
 Bessell M.S., 1990, *PASP* 102, 1181
 Bessell M.S., Castelli F., Plez B., 1998, *A&A* 333, 231
 Blackwell D.E., Lynas-Gray A.E., 1994, *A&A* 282, 899
 Blackwell D.E., Lynas-Gray A.E., 1998, *A&AS* 129, 505
 Blackwell D.E., Shallis M.J., 1977, *MNRAS* 180, 177
 Böhm-Vitense E., 1982, *ApJ* 255, 191
 Buser R., 1978, *A&A* 62, 411
 Buser R., Kurucz R.L., 1978, *A&A* 70, 555
 Buser R., Kurucz R.L., 1992, *A&A* 264, 557
 Canuto V.M., Mazzitelli I., 1992, *ApJ* 389, 724

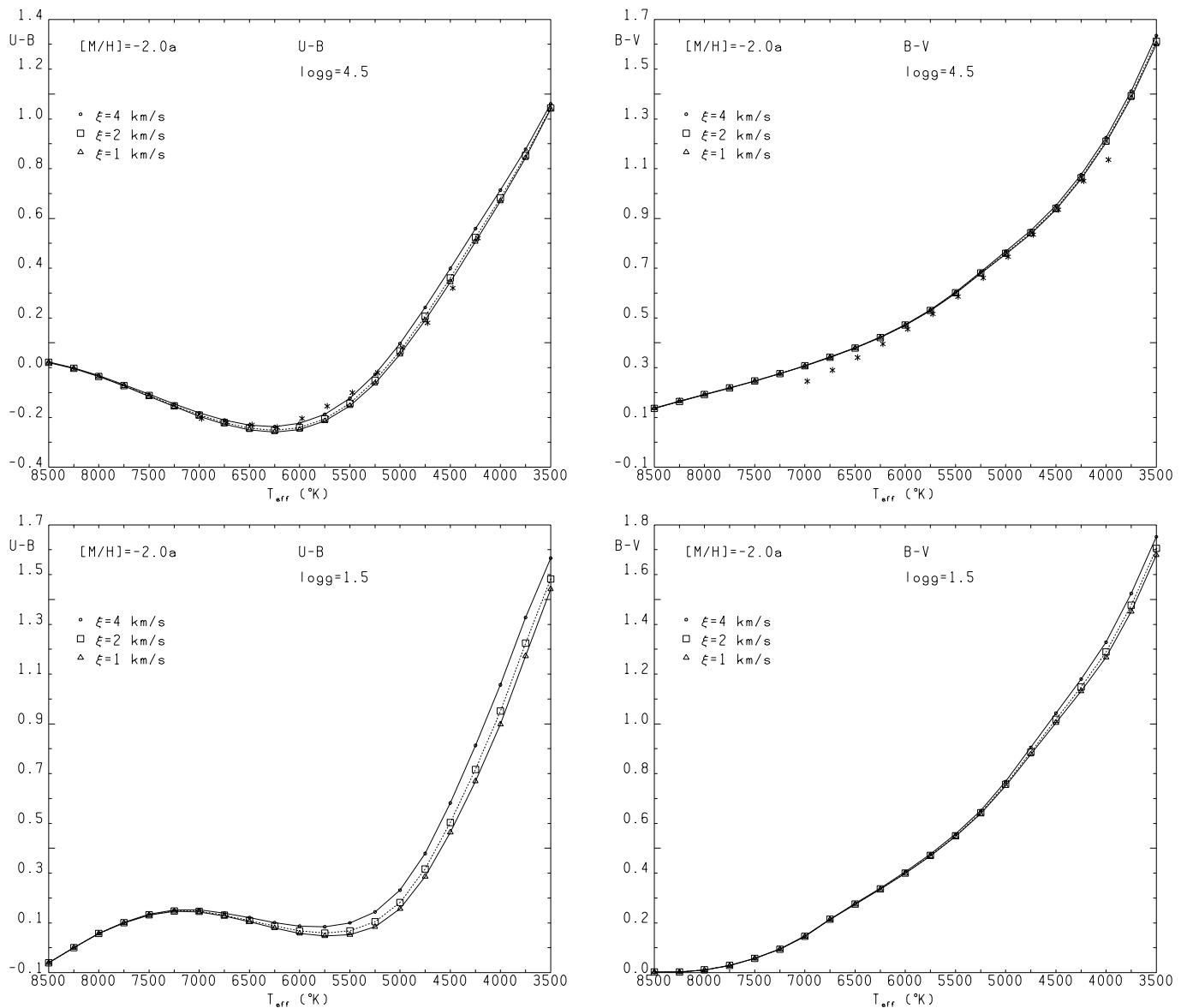


Fig. 23. $T_{\text{eff}}(\text{U-B})$ and $T_{\text{eff}}(\text{B-V})$ relations from models with $[M/H] = -2.0a$ and different microturbulent velocities $\xi = 1, 2,$ and 4 km s^{-1} . The empirical relations from Alonso et al. (1996b) (points) are compared with the relations computed for $\log g = 4.5$. Upper plots are for $\log g = 4.5$, lower plots are for $\log g = 1.5$.

Carney B.W., Latham D.W., 1987, AJ 92, 116

Castelli F., 1996, In: Adelman S.J., Kupka F., Weiss W. (eds.) Proceedings of the Vienna workshop on Model Atmospheres and Spectrum Synthesis. ASP Conference Series 108, p. 85

Castelli F., Kurucz R.L., 1994, A&A 281, 817

Castelli F., Gratton R.G., Kurucz R.L., 1997, A&A 318, 841

Cayrel de Strobel G., 1996, A&AR 7,243

Code A.D., Davis J., Bless R.C., Hanbury Brown R., 1976, ApJ 203, 417

Cousins A.W., 1972, Mon. Notes Astron. Soc. S. Afr. 31,69

Crowther P.A., 1997, in: Bedding T.R., Booth A.J., Davis J. (eds.) Fundamental Stellar Properties: The Interaction between Observation and Theory. IAU Symp. 189, p. 137

Eriksson K., Bell R.A., Gustafsson B., Nordlund A., 1979, Trans. IAU, Vol.17A, Part 2, Reidel, Dordrecht, p. 200

FitzGerald M.P., 1970, A&A 4, 234

Gratton R., Carretta E., Castelli F., 1996, A&A 314, 191

Gray D.F., 1989, FGK Stars and T Tauri Stars. Monograph Series on Nonthermal Phenomena in Stellar Atmospheres. NASDA SP-502, p. 7

Gray D.F., 1995, PASP 107, 120

Gustafsson B., Bell R.A., Eriksson K., Nordlund A., 1975, A&A 42, 407

Hayes D.S., 1985, In: Hayes D.S., Pasinetti L.E., Davis Philip A.G. (eds.) Calibration of Fundamental Stellar Quantities. IAU Symp. 111, p. 225

Holweger H., Kock M., Bard A., 1995, A&A 296, 233

Johnson H.L., Mitchell R.I., Iriarte B., Wisniewski W.Z., 1966, Comm. Lunar Planetary Lab. 4, 99

Johnson H.L., Morgan W.W., 1951, ApJ 114, 522

Kurucz R.L., 1979, ApJS 40, 1

- Kurucz R.L., 1991, In: Philip A.G., Davis, Upgren A.R., Janes K.A. (eds.) Precision Photometry: Astrophysics of the Galaxy. p. 27
- Kurucz R.L., 1992, In: Barbuy B., Renzini A. (eds.) Stellar Populations of Galaxy. IAU Symp. 149, p. 252
- Kurucz R.L., 1993a, CD-ROM No. 13
- Kurucz R.L., 1993b, CD-ROMs No. 2, No. 3, No. 4
- Kurucz R.L., 1994, CD-ROM No. 19
- Kurucz R.L., 1995, CD-ROM No. 13, revised
- Kurucz R.L., 1997a, private communication
- Kurucz R.L., 1997b, In: Bedding T.R., Booth A.J., Davis J. (eds.) Fundamental Stellar Properties: The Interaction between Observation and Theory. IAU Symp. 189, p. 217
- Kurucz R.L., Peytremann, E., 1975, Smithsonian Astrophys. Obs. Special Rep. No 362
- Lejeune Th., Cuisinier F., Buser R., 1997, A&AS 125, 229
- Mégessier C., 1994, A&A 289, 202
- Neckel H., 1994, In: Pap J.M., et al. (eds.) The Sun as a variable Star. IAU Coll. 143, Cambridge Univ. Press, 187
- Schmidt-Kaler Th., 1982, In: Schaifers K., Voigt H.H. (eds.) Landolt-Börnstein, Neue Serie, Gruppe VI, Bd 2b, Springer, p. 14
- Ryan S.G., 1989
- Sandage A., Kowal C., 1986, AJ 91, 1140
- Straizys V., Sviderskiene Z., 1972, Bull. Vilnius Astron. Obs. 35
- Tüg, H., Schmidt-Kaler T., 1982, A&A 105, 400
- Warren Jr. W.H., Hoffleit, D., 1994, The Bright Stars Catalogue, 5th revised edition, Nasa Goddard Space Flight Center